RESEARCH ARTICLE

TORC2 inhibition of α-arrestin Aly3 mediates cell surface persistence of *S. pombe* Ght5 glucose transporter in low glucose

Yusuke Toyoda, Saeko Soejima, Fumie Masuda and Shigeaki Saitoh*

ABSTRACT

In the fission yeast, *Schizosaccharomyces pombe*, the high-affinity hexose transporter, Ght5, must be transcriptionally upregulated and localized to the cell surface for cell division under limited glucose. Although cell-surface localization of Ght5 depends on Target of rapamycin complex 2 (TORC2), the molecular mechanisms by which TORC2 ensures proper localization of Ght5 remain unknown. We performed genetic screening for gene mutations that restore Ght5 localization on the cell surface in TORC2-deficient mutant cells, and identified a gene encoding an uncharacterized α-arrestin-like protein, Aly3/SPCC584.15c. α-arrestins are thought to recruit a ubiquitin ligase to membrane-associated proteins. Consistently, Ght5 is ubiquitylated in TORC2-deficient cells, and this ubiquitylation is dependent on Aly3. TORC2 supposedly enables cell-surface localization of Ght5 by preventing Aly3-dependent ubiquitylation and subsequent ubiquitylation-dependent translocation of Ght5 to vacuoles. Surprisingly, nitrogen starvation, but not glucose depletion, triggers Aly3-dependent transport of Ght5 to vacuoles in *S. pombe*, unlike budding yeast hexose transporters, vacuolar transport of which is initiated upon changes in hexose concentration. This study provides new insights into the molecular mechanisms controlling the subcellular localization of hexose transporters in response to extracellular stimuli.

KEY WORDS: Glucose limitation, Nitrogen starvation, Hexose transporter, Ubiquitylation, Target of rapamycin complex, Arrestin

INTRODUCTION

Eukaryotic cells monitor the nutritional status of their micro-environments and modulate metabolic processes in response to changes in nutrient availability. The fission yeast *Schizosaccharomyces pombe* possesses eight genes encoding hexose transporters ($ght1^+$ – $ght8^+$), through which glucose, fructose and their derivatives are transported across the cell membrane (Heiland et al., 2000; Wood et al., 2002). The high-affinity transporter Ght5 is required for cell proliferation under limited glucose. Expression levels and localization of Ght5 are regulated in response to the hexose concentration. Although $ght5^+$ transcription is repressed in wild-type cells growing in conventional laboratory medium with a high concentration of glucose (111-167 mM/2-3%), when glucose is limited, its transcription level is greatly increased in a manner dependent on Ca^{2+}/calmodulin-dependent-kinase kinase (CaMKK)

Department of Cell Biology, Institute of Life Science, Kurume University, Asahi-machi 67, Kurume, Fukuoka 830-0011, Japan.

*Author for correspondence (saitou_shigeaki@kurume-u.ac.jp)

Y.T., 0000-0003-0534-6898; S.S., 0000-0001-5408-296X

and AMP-dependent kinase (AMPK) (Saitoh et al., 2015). In cells growing in conventional high-glucose medium, Ght5 protein, which is expressed at a low level, localizes on the cell surface, preferentially near the cell equator, whereas abundantly expressed Ght5 is distributed across the entire cell surface in low-glucose (4.4 mM) medium (Saitoh et al., 2015). Target of rapamycin kinase complex 2 (TORC2) and its downstream kinase, Gad8, are essential for proper localization of Ght5 on the cell membrane.

TOR kinases form two distinct evolutionarily conserved complexes, TORC1 and TORC2 (Wullschleger et al., 2006). TORC1 consists of a catalytic subunit, which is encoded by the $tor2^+$ gene in *S. pombe*, and regulatory subunits, including Raptor, encoded by the *S. pombe* $mip1^+$ gene. TORC2 consists of a catalytic subunit encoded by the $tor1^+$ gene and regulatory subunits, including Rictor, encoded by the $ste20^+$ gene (Hayashi et al., 2007). Activity of TORC1 is regulated through a signaling network, including two GTPases, Rheb (Rhb1 in *S. pombe*) and Rag (Gtr1 and Gtr2 in *S. pombe*), in response to changes in amino acid availability. Rag recruits TORC1 to vacuole membranes, where Rheb binds to and activates TORC1 (Long et al., 2005; Sancak et al., 2010). Activities of Rheb and Rag are controlled positively and negatively by a guanine nucleotide exchange factor (GEF) and a GTPase-activating protein (GAP), respectively. The Tsc1-Tsc2 protein complex functions as a GAP for Rheb, whereas the Ragulator complex and the GATOR1 complex function as GEF and GAP for Rag, respectively (Bar-Peled et al., 2013, 2012; Tee et al., 2003; Zhang et al., 2003). Activated TORC1, in the presence of amino acids, promotes various cellular processes, such as protein translation, ribosome biogenesis, transcription and autophagy inhibition (Barbet et al., 1996; Powers and Walter, 1999). On the other hand, TORC2 is activated upon stimulation with insulin, and regulates glucose metabolism, actin organization and cell survival in mammals (Saxton and Sabatini, 2017). A major effector kinase functioning downstream of TORC2 is Akt, which is activated by TORC2 in coordination with phosphoinositide-dependent protein kinase 1 (PDK1) (Alessi et al., 1997; Sarbassov et al., 2005; Stokoe et al., 1997). In fission yeast, the TORC2 signaling cascade is essential for cell proliferation under low-glucose conditions. In mutant cells defective for TORC2, Gad8 (the *S. pombe* counterpart of Akt) or Ksg1 (PDK1 in *S. pombe*), the Ght5 hexose transporter, which is essential for uptake of glucose when concentrations are low, is not localized on the cell surface properly (Niederberger and Schweingruber, 1999; Saitoh et al., 2015; Tatebe and Shiozaki, 2010).

When no longer required, cell-surface proteins, e.g. receptor and transporter proteins, are internalized by endocytosis (Antonescu et al., 2014). During endocytosis, a small part of the plasma membrane along with the membrane-associated proteins forms a pit and then buds inward to form a vesicle, which fuses with other vesicles to form endosomes in the cytoplasm. Proteins (i.e. cargos)

on such vesicles/endosomes are either transported back to the cell surface by exocytosis or transported to lysosomes (or vacuoles in yeasts) for degradation (Sorkin, 2000). The destination of vesicular cargos is determined by protein ubiquitylation, which is mediated by E3 ubiquitin ligases that ubiquitylate substrate proteins, and arrestin proteins, bridging the ligases and the cargos (Clague et al., 2012). Ubiquitylated cargos are sorted for transport to lysosomes/ vacuoles by conserved protein complexes known as endosomal sorting complexes required for transport (ESCRTs) (Katzmann et al., 2001; Vietri et al., 2020). On membranes of endosomes and/or multivesicular bodies (MVBs), ubiquitylated cargos are first captured by the multivalent ubiquitin-binding complex, called ESCRT-0. Through actions of ESCRT-I, ESCRT-II and ESCRT-III complexes, ubiquitylated cargos are then gathered along a small portion of the cell membrane, which buds into the lumen of the endosome, forming MVBs. These MVBs fuse with lysosomes to be degraded. As arrestins determine which cargos are connected with ubiquitin ligases (Becuwe et al., 2012a; Nikko and Pelham, 2009), they apparently serve crucial functions in determining the endocytic destinations of the cargos.

Arrestin-family proteins are evolutionarily conserved among eukaryotes, from yeasts to humans (Alvarez, 2008). Arrestin was originally identified as a protein involved in the termination of the signal from the light-activated photoreceptor, rhodopsin (Wilden et al., 1986; Zuckerman and Cheasty, 1986). Arrestin-family proteins, which are classified into four subfamilies, α-arrestins, β-arrestins, visual arrestins and Vps26-related proteins, serve in various capacities, including as adaptors connecting NEDD4-like E3 ubiquitin ligases to membrane-associated substrates (Alvarez, 2008; Becuwe et al., 2012a). According to annotations in the fission yeast genome database [Pombase (Lock et al., 2019), www. pombase.org/term/PBO:0000342], 11 genes (*aly1+*, *aly2+*, *any1+*, *any2+*, *art1+*, *mug170+*, *rod1+*, *ste7+*, *vps26+*, SPBC557.05 and SPCC584.15c) encode proteins containing one or more arrestin-related domains (InterPro ID: IPR011021, IPR011022, IPR014752 and IPR024391; Mitchell et al., 2019) (Fig. 3A). Among them, four genes, *aly1+*, *aly2+*, *rod1+* and SPCC584.15c, encode proteins with domains and motifs typical of α-arrestin subfamily proteins: arrestin-like N-terminal and C-terminal domains (InterPro ID: IPR011021 and IPR011022) and multiple PY motifs at the C-terminal tail region (Fig. 3A; Puca and Brou, 2014). One of the fission yeast arrestin-family proteins, Any1, is reportedly essential for ubiquitylation of an amino acid transporter, Aat1, and its retention at Golgi bodies (Nakase et al., 2013). Interaction between Any1 and a NEDD4-like E3 ubiquitin ligase, Pub1, is stabilized by activation of the Rheb GTPase, Rhb1, which promotes ubiquitylation of Aat1 so as to prevent trafficking of Aat1 from the Golgi to the cell surface. To date, none of the four α-arrestin genes mentioned above has been experimentally characterized.

Molecular functions of arrestins have been well studied in the budding yeast *Saccharomyces cerevisiae*. Among 14 budding yeast α-arrestins, Csr2, Rod1, and Rog3 regulate trafficking of hexose transporters from the plasma membrane to vacuoles in response to changes in glucose concentration (Becuwe et al., 2012b; Hovsepian et al., 2017; Nikko and Pelham, 2009; O'Donnell et al., 2015). Under glucose-rich conditions, these α-arrestins mediate ubiquitylation of hexose transporters on the plasma membrane by Rsp5 ubiquitin ligase. When the concentration of glucose is reduced, activated AMPK phosphorylates these α-arrestins and downregulates them, so that hexose transporters are retained on the cell surface. Phosphorylation by AMPK prevents these α-arrestins from associating with hexose transporters on the cell surface

(O'Donnell and Schmidt, 2019). Rod1, phosphorylated by AMPK, is subjected to protein degradation and/or binding to the 14-3-3 protein Bmh2 (Llopis-Torregrosa et al., 2016; O'Donnell et al., 2015).

In this study, to understand how TORC2 ensures proper localization of the Ght5 hexose transporter in fission yeast, we performed genetic screening for suppressor mutations that restore Ght5 localization on the cell surface in TORC2-deficient cells. Genetic and biochemical analyses indicate that Ght5 is ubiquitylated in a manner dependent on a specific α-arrestin, Aly3/Spcc584.15c, and that ESCRT complexes apparently sort ubiquitylated Ght5 to vacuoles. Importantly, combined with results reported in our previous study (Saitoh et al., 2015), our findings strongly suggest that TORC2, but probably not AMPK, inhibits Aly3-dependent ubiquitylation of Ght5, and consequently blocks endocytosis of Ght5 to vacuoles. Unlike budding yeast, nitrogen starvation (no ammonium ion or amino acids), but not glucose repletion, triggers Aly3-dependent endocytosis of Ght5 to vacuoles in fission yeast. Our studies demonstrate that glucose uptake via the high-affinity hexose transporter Ght5 is cross-regulated by levels of hexoses and nitrogen-containing compounds, and that TORC2 is central to this unique regulation of nutrient uptake.

RESULTS
Isolation of extragenic suppressors of the *gad8ts* mutant

In fission yeast, the TORC2 kinase signaling pathway is essential for proper localization of the high-affinity hexose transporter Ght5 on the plasma membrane. Mutant cells defective in TORC2 or Gad8 kinase, which acts downstream of TORC2, exhibited abnormal accumulation of Ght5 in the cytoplasm, and consequently failed to proliferate in low glucose (Saitoh et al., 2015). To understand how the TORC2 signaling pathway ensures the proper localization of Ght5 and cell proliferation in low glucose, we screened for extragenic suppressor mutations enabling *gad8ts* cells, which harbor a temperature-sensitive mutation (S240P) in the *gad8+* gene, to proliferate on low-glucose medium containing 3.3 mM glucose. When incubated on solid low-glucose medium at 33°C, *gad8ts* cells spontaneously acquired a suppressor mutation, and formed colonies at a frequency of 370 in 1×10^7 cells (Fig. 1A). A total of 49 colonies on low-glucose medium were then selected, and whole genome sequences of these cells were analyzed to identify the mutated gene. Mutations in 32 genes were identified as candidates for the extragenic suppressor.

To confirm that the identified mutations ameliorated proliferation of *gad8ts* mutant cells in low glucose, each of the 32 identified genes was deleted in *gad8ts* mutant cells. Among them, deletion of 22 genes improved proliferation of *gad8ts* mutant cells in low glucose compared to the parental *gad8ts* mutant (Fig. 1B; Fig. S1), suggesting that a loss-of-function mutation of these genes suppresses the growth defect phenotype of *gad8ts* cells in low glucose. Notably, although most strains proliferated well in high glucose (167 mM), *gad8ts* cells lacking the *gtr1+* or *npr2+* gene failed to form colonies. Chia et al. (2017) thought that this defect was due to impaired amino acid uptake. As these mutant cells formed colonies on low-glucose plates, reduction of the glucose concentration may somehow enhance amino acid uptake.

Based on annotated/inferred gene functions, the 22 extragenic suppressor genes, the deletion of which restored cell proliferation in low glucose, were classified into four groups (Table 1). The first group of mutations was supposed to block endocytosis of plasma membrane proteins. *sst4+*, *hse1+*, *sst6+*, *vps25+* and *bro1+* encode components of the ESCRT machinery, which is required for

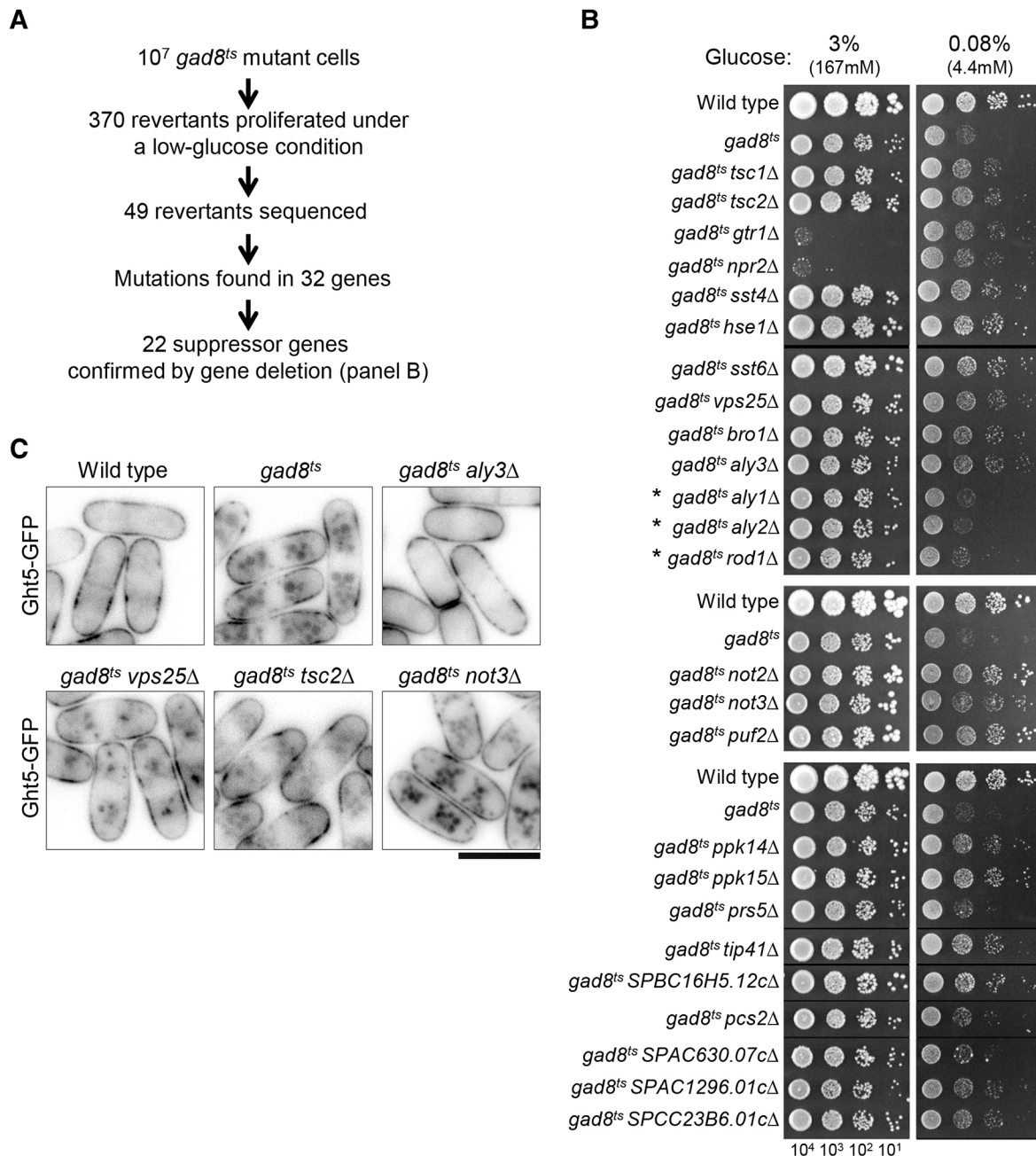**Fig. 1. Identification of extragenic suppressors of the gad8^ts mutant.** (A) Schematized procedure for obtaining extragenic suppressor mutations of the gad8^ts mutant. (B) Aliquots (10^4 cells) of wild-type, gad8^ts mutant and gad8^ts mutant strains lacking the indicated genes were serially diluted 10-fold, spotted onto YES solid medium containing the indicated concentration of glucose, and incubated for 5 days at 33°C. Spots from the same square Petri dishes are shown on a black background. See also Fig. S1. Genes with asterisks (aly1^+, aly2^+ and rod1^+) are related to the identified arrestin-like gene, SPCC584.15c/aly3^+. (C) Subcellular localization of Ght5 in living wild-type, gad8^ts mutant and gad8^ts mutant cells lacking the indicated genes. Cells expressing Ght5-GFP were cultivated in EMM2 containing 0.06% glucose for 4 h at 33°C. See also Fig. S2. Scale bars: 10 μm.

transport of the transmembrane Aat1 protein to vacuoles (Nakase et al., 2012). *SPCC584.15c* encodes an α-arrestin-like protein inferred to be involved in ubiquitin-dependent endocytosis of membrane-associated proteins (Lock et al., 2019), referred to hereafter as *aly3^+* (arrestin-like protein in *y*east 3). The second group of suppressor genes appear to be involved in the TORC1 kinase signaling pathway. Mutations in *tsc1^+*, *tsc2^+*, *gtr1^+* and *npr2^+* are thought to enhance TORC1 activity in *S. pombe* (Chia et al., 2017; Fukuda and Shiozaki, 2018; Manning and Cantley, 2003; Tee et al., 2003). The *tip41^+* gene encodes a type-2A protein phosphatase regulator, a homolog of which downregulates the TORC1 signaling

pathway in budding yeast (Fenyvuesvolgyi et al., 2005; Jacinto et al., 2001). The third group of suppressors appears to be involved in RNA metabolism. *not2^+* and *not3^+* encode subunits of the CCR4-NOT complex, which is primarily involved in mRNA deadenylation (Ukleja et al., 2016), and the fission yeast *puf2^+* gene encodes an RNA-binding protein belonging to the Pumilio and FBF family, which is required to form stress granules after deprivation of glucose (Hsiao et al., 2020). The fourth group contains genes with miscellaneous functions not classified above. *ppk14^+* and *ppk15^+* encode protein kinases. *prs5^+* encodes a ribose-phosphate pyrophosphokinase involved in nucleotide synthesis. *pcs2^+*

Table 1. Extragenic suppressors of *gad8*^{ts} mutant

Mutant gene	Product	Mutation site
Endocytosis to vacuoles		
sst4	sorting receptor for ubiquitylated membrane proteins, ESCRT 0 complex subunit Sst4	W170Stop, Q202Stop
hse1	STAM like protein Hse1	#
sst6	ESCRT I complex subunit Vps23	Q207Stop, %
vps25	ESCRT II complex subunit Vps25	W113Stop
bro1	BRO1 domain protein Bro1	E644Stop
SPCC584.15c (*aly3*)	arrestin involved in ubiquitin-dependent endocytosis	R457Stop
TORC1 signaling pathway		
tsc1	hamartin	Q688Stop
tsc2	tuberin	L636Stop
gtr1	Gtr1/RagA G protein Gtr1	C58F
npr2	SEA/Iml1/Npr2/3 complex subunit Npr2	Q135K
tip41	TIP41-like type 2a phosphatase regulator Tip41	R165L
RNA metabolism		
not2	CCR4-Not complex subunit Not2	E31Stop, #
not3	CCR4-Not complex subunit Not3/5	#
puf2	pumilio family RNA-binding protein Puf2	Q40Stop, Y416Stop, R751P, R751C, I810S
Miscellaneous		
ppk14	serine/threonine protein kinase Ppk14	R148Stop, D404E, R469L
ppk15	serine/threonine protein kinase Ppk15	N104T, K259N
prs5	ribose-phosphate pyrophosphokinase Prs5	L23I
SPBC16H5.12c	DUF2433 metallo phosphatase superfamily conserved fungal protein	L67P
pcs2	phytochelatin synthetase	N147D
SPAC1296.01c	phosphoacetylglucosamine mutase	Q175Stop
SPAC630.07c	*Schizosaccharomyces* specific protein	P278T
SPCC23B6.01c	oxysterol binding protein	S117Stop

\# indicates 'splice region variant and intron variant'.
% indicates 'splice acceptor variant, splice donor variant and intron variant'.

encodes a phytochelatin synthetase involved in the detoxification of heavy metals, and *SPBC16H5.12c* encodes a protein with a metal-dependent phosphatase-like superfamily domain (see Table 1). Collectively, the proliferation defect caused by TORC2 deficiency in low glucose was rescued by loss-of-function mutations in the ESCRT/endocytosis machinery, the TORC1 signaling pathway and RNA metabolism. The TORC2-Gad8 signal may block functions of these genes directly or indirectly to enable cell proliferation in low glucose.

Mutations in the ESCRT machinery and Aly3 α-arrestin effectively restore cell-surface localization of Ght5 in *gad8*^{ts} mutants

We then tested whether deletion of the suppressor genes restored not only cell proliferation, but also Ght5 localization in *gad8*^{ts} mutant cells. Using *S. pombe* cells in which the native *ght5*⁺ gene was replaced with that for the C-terminally GFP-fused Ght5 protein (Ght5-GFP), subcellular localization of Ght5 was examined after cultivation for 4 h in low glucose (Fig. 1C; Fig. S2). Although Ght5-GFP was intensely evident on the cell surface in wild-type cells, it accumulated predominantly in the cytoplasm and only weakly on the cell membrane in *gad8*^{ts} mutant cells, as reported previously (Saitoh et al., 2015). As Ght5-GFP localized inside the vacuole, the membrane of which was visualized by a vacuole-marker, FM4-64, in *tor1Δ* mutant cells, which lacked the catalytic component of TORC2, essential for the activation of Gad8 (Fig. 2A,B), cytoplasmic Ght5-GFP in the *gad8*^{ts} cells was supposed to locate in vacuoles. Compared to the parental *gad8*^{ts} single-mutant cells, *gad8*^{ts} cells with deleted suppressor genes exhibited reduced Ght5-GFP signals in the cytoplasm and a stronger signal on the cell surface, although the extent of the recovery of Ght5 localization varied among strains. Most strikingly, in *gad8*^{ts} cells with the deleted *aly3*⁺ gene (*gad8*^{ts} *aly3Δ*), virtually no GFP signals were detectable in the cytoplasm, indicating that deletion of the *aly3*⁺

gene almost fully suppressed the abnormal cytoplasmic accumulation of Ght5 due to the TORC2 deficiency (Fig. 1C). Deletion of genes for the ESCRT machinery effectively restored Ght5-GFP localization on the cell surface, though characteristic Ght5-GFP puncta, which appeared different from the vacuoles, remained in the cytoplasm. Deletion of TORC1 signaling pathway genes (*tsc1*, *tsc2*, *gtr1* and *npr2*) also largely restored Ght5-GFP on the cell surface, and small, but significant, amounts of Ght5 remained in vacuoles. In contrast, deletion of suppressor genes involved in RNA metabolism, *not2*⁺, *not3*⁺ and *puf2*⁺, scarcely suppressed accumulation of Ght5-GFP in vacuoles, although it did effectively restore cell proliferation of *gad8*^{ts} cells in low-glucose medium (see Fig. 1B,C; Fig. S2).

Aly3 is the only canonical α-arrestin that regulates Ght5 endocytosis to vacuoles

As shown above, among the identified 22 suppressor genes, *aly3*⁺ was the strongest suppressor, deletion of which fully restored Ght5-GFP localization on the cell surface in *gad8*^{ts} mutant cells (see Fig. 1C). Therefore, we focused on *aly3*⁺ and closely related arrestin genes for further analyses. Although *aly3*⁺ has been identified in systematic screens for genes affecting the toxicity of an anti-cancer drug, bortezomib, and genes affecting cell morphology during the mating process (Dudin et al., 2017; Takeda et al., 2011), its physiological role remained unknown. *aly3*⁺ encodes a protein containing arrestin-like N- and C-terminal domains and two proline-rich PY motifs, which are characteristic of canonical α-arrestin proteins (Fig. 3A; Puca and Brou, 2014). Although Aly3 protein is annotated as an ortholog of human α-arrestins in the fission yeast genome database (Lock et al., 2019), the amino acid sequence similarity of *S. pombe* Aly3 and human α-arrestins was relatively low. For example, amino acid identity along the entire length of *S. pombe* Aly3 and its closest human homolog, ARRDC2, is 22% (Fig. 3A,B). In the *S. pombe* genome, three more genes encode
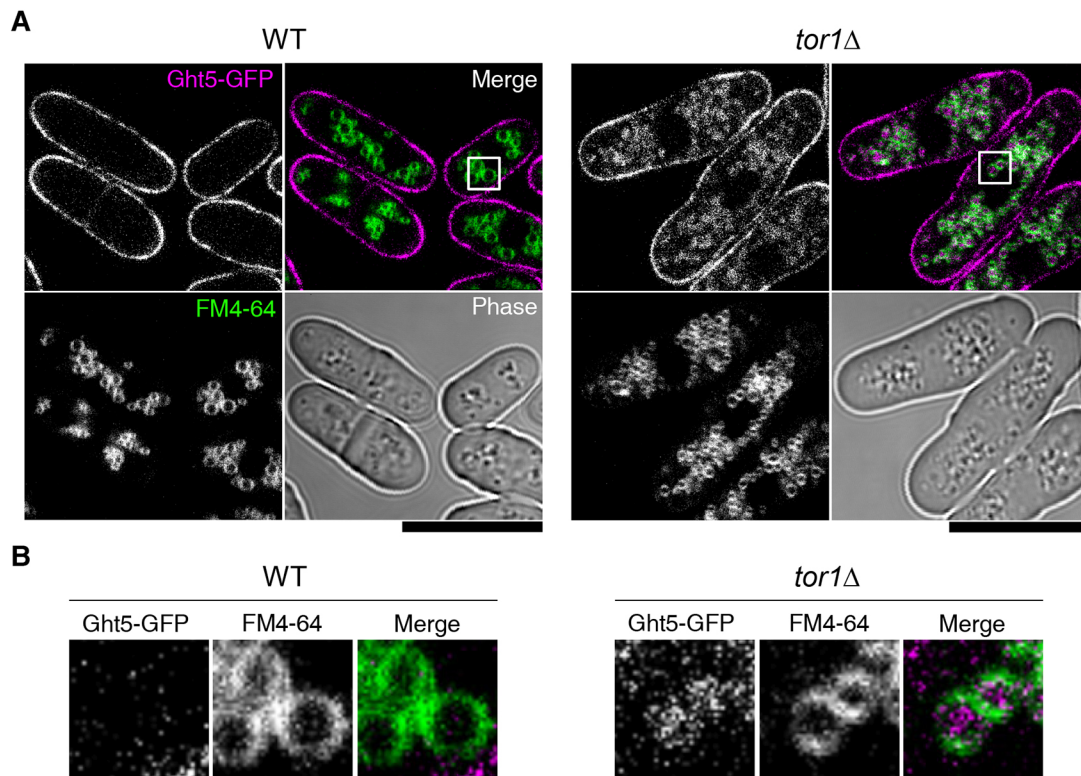
Fig. 2. Vacuolar localization of Ght5 in TORC2-defective *tor1Δ* cells. (A) Wild-type (WT) and *tor1Δ* cells expressing Ght5-GFP were cultivated in EMM2 containing 4.4 mM glucose at 33°C for 4 h, and were stained with FM4-64. Confocal images of Ght5-GFP (upper left, magenta in merged images), FM4-64 (lower left, green), phase-contrast (lower right) and merged (upper right) images are shown. Scale bars: 10 μm. (B) Enlarged (4.5×) images of the boxed area of the merged images in A.

Aly3-like proteins, which harbor these domains and motifs in the same configuration as in Aly3. Thus, we examined whether these four α-arrestins, Aly1, Aly2, Aly3 and Rod1, redundantly regulate endocytosis of Ght5 to vacuoles. For this purpose, we constructed *gad8*[ts] mutant strains in which one of these four α-arrestin genes was disrupted, and tested whether these double-mutant cells could proliferate in low glucose. Notably, although deletion of *aly3*[+] enabled *gad8*[ts] cells to form colonies in low glucose, deletion of the other three α-arrestin genes had little or no effect (Fig. 1B; Fig. S1). Consistently, deletion of α-arrestin genes other than *aly3*[+] failed to restore localization of Ght5 on the cell surface in *gad8*[ts] cells. Intense cytoplasmic GFP signals were observed in *gad8*[ts] *aly1Δ*, *gad8*[ts] *aly2Δ* and *gad8*[ts] *rod1Δ* double-mutant cells (Fig. 3C). Collectively, these results suggested that among these four α-arrestins, only Aly3 is involved in Ght5 endocytosis to vacuoles. Aly3 potentially promotes endocytosis of Ght5 from the surface, and the TORC2-Gad8 signaling pathway counteracts Aly3 to ensure retention of Ght5 on the cell surface.

Endocytosis of the Ght5 hexose transporter is triggered by nitrogen depletion but not by glucose starvation

The results described above imply that wild-type fission yeast cells possess a mechanism to remove Ght5 transporters from the surface by endocytosis, and that Aly3 and the counteracting TORC2 regulate this mechanism. These findings raise the question of what cue initiates endocytosis of Ght5. In budding yeast, endocytosis of hexose transporters from the plasma membrane is reportedly triggered by changes in glucose concentration (Nikko and Pelham, 2009). To test the hypothesis that Ght5 is endocytosed from the cell surface upon glucose repletion, intracellular

localization of Ght5-GFP was examined in *S. pombe* wild-type cells transferred from low-glucose to high-glucose media. Wild-type cells expressing Ght5-GFP from the authentic genomic locus were cultivated in low-glucose Edinburgh minimal medium (EMM2) (4.4 mM glucose) for 10 h, and were then transferred to high-glucose medium with 111 mM glucose (Fig. 4A). Contrary to our hypothesis, Ght5 did not translocate from the surface to vacuoles after the transfer to high-glucose medium. The fluorescence intensity of Ght5-GFP on the cell surface, especially on the growing cell tips, gradually decreased as the cells grew and divided in high-glucose medium, in which Ght5 expression is repressed. However, Ght5 did not accumulate in the cytoplasm or vacuoles. Consistently, although immunoblotting against Ght5-GFP revealed that the amount of Ght5-GFP protein gradually decreased in the wild type as well as in *aly3Δ* cells upon replenishment of a high concentration of glucose (Fig. 4B), C-terminal fragments of degraded Ght5 fused with the GFP moiety resistant to proteolysis (Mukaiyama et al., 2009), which should have been generated by proteolysis in vacuoles, were not detected in either wild-type or *aly3Δ* cells. Similarly, endocytosis of Ght5 to vacuoles was not triggered by complete glucose deprivation. In wild-type cells that were transferred from low-glucose medium to EMM2 without glucose, and that were cultivated for 4 h, Ght5-GFP was still observed on the cell surface, but not in vacuoles (Fig. 4C). These results indicate that changes in the medium hexose concentration do not trigger endocytosis of Ght5 to vacuoles in *S. pombe*, unlike in budding yeast, in which glucose repletion and depletion promote endocytosis to vacuoles and subsequent degradation of the hexose transporters Hxt6 and Hxt1, respectively (Llopis-Torregrosa et al., 2016; Roy et al., 2014).
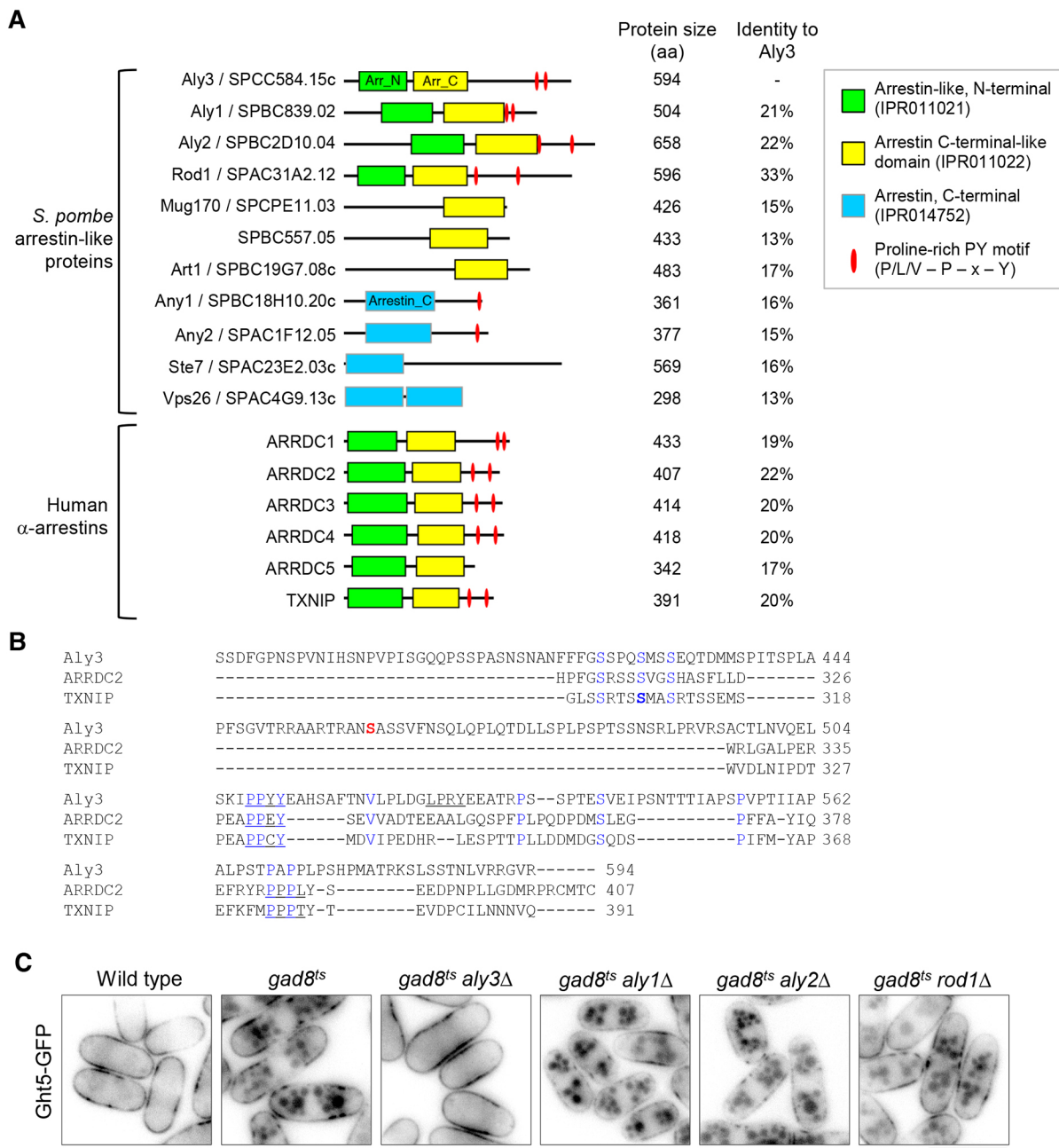
Fig. 3. Aly3 is the only α-arrestin that regulates Ght5 endocytosis to vacuoles. (A) Structure of 11 *S. pombe* proteins containing one or more arrestin-related domains and human α-arrestin proteins. Green (IPR011021), yellow (IPR011022) and blue (IPR014752) boxes indicate arrestin-related domains with distinct InterPro IDs. Red bars indicate the proline-rich PY motif. For each protein, the amino acid length and identity to Aly3 are shown. (B) Alignment of the carboxyl terminal region of Aly3, ARRDC2 and TXNIP proteins. Amino acid sequences of *S. pombe* Aly3, human ARRDC2 and TXNIP from the C-terminal end of the arrestin C-terminal-like domain to the carboxyl terminus were aligned using Clustal Omega. A part of the Aly3 sequence (residues 325 to 384) is not shown because no amino acids of ARRDC2 or TXNIP were aligned. Conserved amino acid residues are in blue. The 308th serine residue of TXNIP is in bold, and the 460th serine residue of Aly3 is in bold and red. PY motifs are underlined. (C) Subcellular localization of Ght5 in living wild-type, *gad8*ts mutant and *gad8*ts mutant cells lacking the α-arrestin genes. Cells expressing Ght5-GFP were cultivated in EMM2 containing 0.06% glucose for 4 h at 33°C. Scale bar: 10 μm.

Unexpectedly, depletion of ammonium chloride (NH_4Cl), the sole nitrogen source in the medium, triggered endocytosis of Ght5 to vacuoles. Wild-type and *aly3Δ* cells expressing Ght5-GFP were cultivated in low-glucose EMM2, which contained 0.5% (93.4 mM) NH_4Cl, for 10 h, before being transferred to ammonium-depleted low-glucose medium (Fig. 5A). In wild-type cells, the fluorescence intensity of Ght5-GFP gradually decreased on the cell surface after the transfer to ammonium-depleted medium, and instead, Ght5-GFP fluorescence in cytoplasmic vacuoles became prominent. At 6 h after depletion of NH_4Cl, Ght5-GFP was detectable only in vacuoles (Fig. 5B). This translocation of Ght5 upon ammonium starvation was fully dependent on Aly3. In *aly3Δ* cells, Ght5-GFP remained localized predominantly on the cell surface, even 6 h after ammonium removal. Aly3-dependent translocation of Ght5 to vacuoles upon ammonium starvation was also observed in high glucose (Fig. 5C).
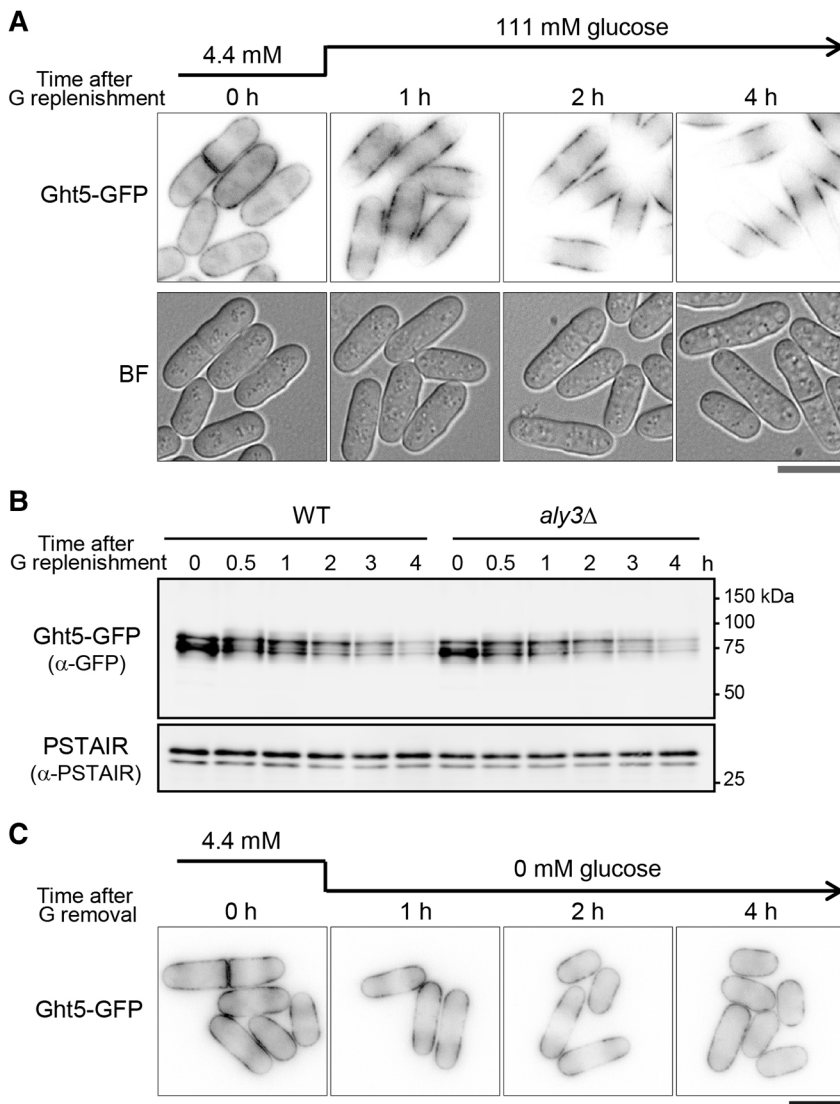
Fig. 4. Depletion or replenishment of glucose in the medium does not induce Ght5 endocytosis to vacuoles. (A,B) Cells expressing Ght5-GFP were pre-cultured in low-glucose (4.4 mM) EMM2 at 33°C for 10 h. At time 0 h, cells were transferred to EMM2 containing 111 mM glucose (denoted as G), and aliquots were taken at the indicated time points for imaging Ght5-GFP in wild-type (WT) cells (A) and for the detection of Ght5-GFP in wild-type and $aly3\Delta$ cells by immunoblotting (B). BF denotes brightfield images. PSTAIR was used as a loading control. (C) wild-type cells expressing Ght5-GFP were pre-cultured in low-glucose EMM2 at 33°C for 10 h. At time 0 h, cells were transferred to EMM2 without glucose, and small aliquots were taken at the indicated time points for imaging Ght5-GFP. Scale bars: 10 µm.

Collectively, these observations indicate that endocytosis of the fission yeast Ght5 to vacuoles was regulated in response to changes in the nitrogen concentration (NH_4Cl), but not glucose. It should be noted that leucine starvation in *leu1-32* auxotroph mutants also caused translocation of Ght5 to vacuoles (Fig. 5D), even in the presence of 93.4 mM NH_4Cl. Thus, amino acid starvation caused by nitrogen depletion is likely the direct trigger for Ght5 translocation.

Aly3-dependent translocation of Ght5 to vacuoles appears to be important for cells to survive nitrogen starvation. Wild-type and *aly3Δ* cells were pre-incubated in low-glucose EMM2 supplemented with 93.4 mM NH_4Cl for 10 h, and cell viability was measured after the transfer to low-glucose ammonium-depleted EMM2 (Fig. 5E; Fig. S3A). Although wild-type cells maintained high viability (>60%) for 7 days, the viability of *aly3Δ* cells decreased to 36.3% in 5 days, and to 32.2% 7 days after the transfer. Proteolysis of Ght5 protein endocytosed to vacuoles may regenerate the cellular amino acid pool at the cost of high-affinity glucose uptake to extend cellular chronological lifespan under nitrogen starvation.

These results prompted us to examine whether *aly3⁺* expression is upregulated upon glucose or nitrogen starvation. For this purpose, mRNA levels of *aly3⁺* were determined by reverse transcription-quantitative PCR (RT-qPCR). First, to test the effect of glucose limitation on *aly3⁺* expression, wild-type cells growing exponentially in high-glucose EMM2 were transferred to and further cultivated in low-glucose EMM2 for 10 h (columns 1 and 2, Fig. 5F). *aly3⁺* mRNA levels, which were determined before and after the transfer to low-glucose medium, were similar in cells growing in high- and low-glucose conditions, suggesting that changes in glucose concentrations in medium have little or no effect on *aly3⁺* expression as long as nitrogen is plentiful in the medium. Next, we examined whether nitrogen starvation upregulates *aly3⁺* expression. Wild-type cells cultivated in low-glucose medium, which is described above, were split into two and further cultivated in fresh low-glucose medium with or without NH_4Cl for 4 h (columns 3 and 4, Fig. 5F). Incubation in nitrogen-depleted medium for 4 h was sufficient to induce Ght5 translocation to vacuoles (Fig. 5B). *aly3⁺* mRNA levels were not changed before or after an additional 4-h cultivation in low-glucose and nitrogen-replenished medium (columns 2 and 3, Fig. 5F). The *aly3⁺* mRNA level slightly increased after cultivation in nitrogen-depleted medium (columns 2 and 4, Fig. 5F), but the amount of increase was small. Taken together, these results suggest that *aly3⁺* mRNA levels are largely constant despite changes in glucose and nitrogen source concentrations.
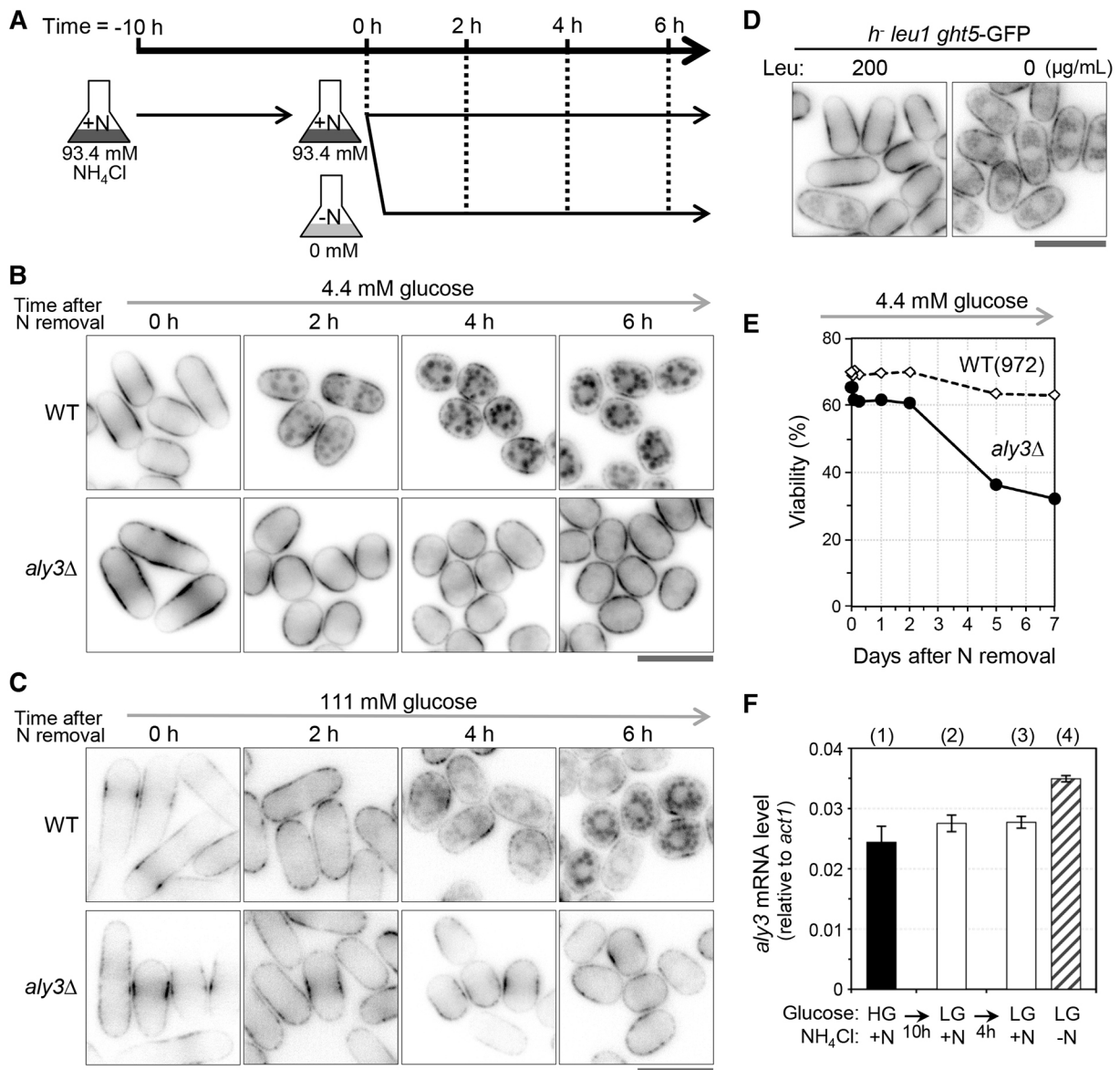
Fig. 5. Aly3-dependent vacuolar transport of Ght5 under nitrogen-starved conditions. (A) Diagram of the experimental procedure for panels B, C, E and F. The glucose concentration of EMM2 is indicated in each panel. Cells expressing Ght5-GFP were pre-cultured in EMM2 containing 0.5% (93.4 mM) ammonium chloride (NH_4Cl) for 10 h at 30°C. At this point, parts of cells were withdrawn as the sample for time=0 h. Remaining cells were transferred to and further cultivated in EMM2 with (+N, panel F) or without NH_4Cl (−N, panels B, C, E and F). N indicates nitrogen sources. (B) Fluorescent images of Ght5-GFP in wild-type (WT) and *aly3Δ* cells under glucose-limited and nitrogen-starved conditions. (C) Fluorescent images of Ght5-GFP in wild-type and *aly3Δ* cells cultivated in nitrogen-deficient EMM2 containing 111 mM glucose. (D) Leucine starvation by *leu1-32* mutation promotes internalization of Ght5. Leucine-auxotroph *leu1-32* mutant cells expressing Ght5-GFP were cultivated in low-glucose EMM2 supplemented with 200 μg/ml leucine for 10 h, and transferred to fresh low-glucose medium with (left panel) or without (right panel) leucine. After an additional 8-h cultivation, fluorescence images of Ght5-GFP were taken. (E) Cell viability under glucose-limited and nitrogen-depleted conditions. Cell culture of wild-type (open diamond) and *aly3Δ* (filled circle) strains was transferred from low-glucose (4.4 mM) and nitrogen-rich EMM2 to low-glucose and nitrogen-deficient EMM2 medium as in panel A, and at the indicated time points after the removal of NH_4Cl, small aliquots of cell culture were withdrawn to measure cell viability. This experiment was repeated twice independently, and the result of the other experiment is presented in Fig. S3A. (F) *aly3+* mRNA levels under various nutritional conditions. Wild-type cells exponentially growing in EMM2 containing 111 mM glucose and 93.4 mM NH_4Cl, parts of which were harvested (HG+N, column 1), were transferred to, and further cultivated in, EMM2 containing 4.4 mM glucose and 93.4 mM NH_4Cl for 10 h (LG+N, column 2). Then, these cells were transferred to, and cultivated in, low-glucose EMM2 with 93.4 mM NH_4Cl (LG+N, column 3) or without the nitrogen source (LG-N, column 4) for 4 h. *aly3+* mRNA levels normalized by that of *act1+* were measured in three biologically independent samples. Data are mean±s.d. The color of the columns indicates the nutritional conditions of the medium: black, 111 mM glucose and 93.4 mM NH_4Cl; white, 4.4 mM glucose and 93.4 mM NH_4Cl; hatched, 4.4 mM glucose and 0 mM NH_4Cl. Scale bars: 10 μm.

TORC2 prevents translocation of Ght5 from the cell membrane to vacuoles by inhibiting Aly3-dependent ubiquitylation under nitrogen-rich conditions

We next investigated how Aly3-dependent endocytosis of Ght5 was inhibited in the presence of nitrogen. The finding that abnormal endocytosis of Ght5 in *gad8ts* mutant cells was fully suppressed by deletion of *aly3+* suggested that Aly3-dependent endocytosis would be inactivated by the TORC2-Gad8 signal under nitrogen-rich conditions. As α-arrestins are thought to recruit an E3 ubiquitin ligase to a transmembrane protein that should undergo endocytosis
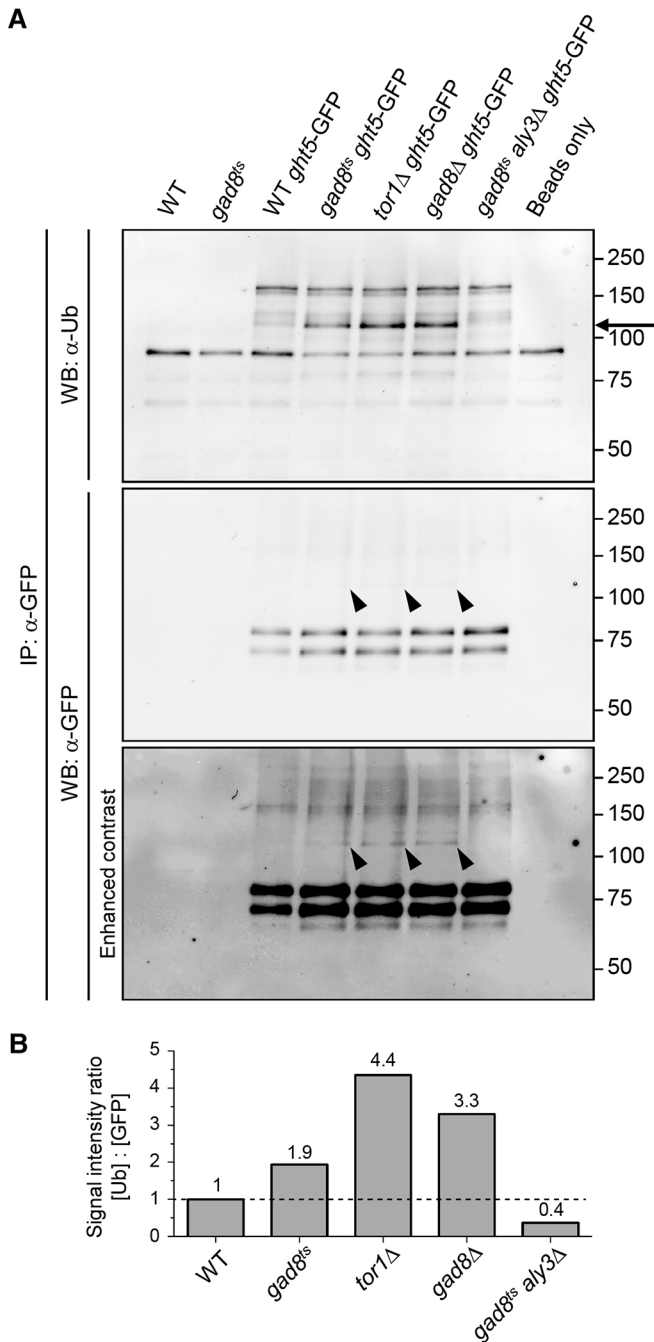
Fig. 6. The TORC2 signaling pathway inhibits Aly3-dependent ubiquitylation of Ght5. (A) Immunoblot of ubiquitylated and total Ght5-GFP in immunoprecipitates. Cell lysates were affinity-purified using anti-GFP antibody-conjugated beads. Blots with anti-ubiquitin (αUb, top panel) and anti-GFP antibodies (αGFP, middle and bottom panels) are shown as ubiquitylated and total Ght5-GFP, respectively. The bottom panel amplifies the contrast in the middle panel. An arrow indicates the band that was more expressed in gad8ts, tor1Δ and gad8Δ mutants than in wild type (WT), but was abolished in the gad8ts aly3Δ mutant. Arrowheads in the middle and bottom panels point to the bands at the same position as the arrow in the top panel. This experiment was repeated three times independently, and results of the other two experiments are presented in Fig. S3B,C. (B) Quantification of ubiquitylated Ght5-GFP protein. Relative signal intensity ratios of ubiquitylated Ght5-GFP protein (indicated by the arrow in panel A) to total Ght5-GFP in the immunoprecipitated fraction are plotted. Signal intensity ratio was normalized using that for wild type. A dashed line indicates the normalized ratio for wild type. A representative result of three independent experiments is shown.

to vacuoles (Puca and Brou, 2014), we hypothesized that Aly3-dependent ubiquitylation of Ght5 would be regulated by the TORC2 signaling pathway. To test this hypothesis, ubiquitylation status of Ght5 was examined in wild-type cells, TORC2-deficient mutant cells and TORC2-deficient $gad8^{ts}$ mutant cells rescued by $aly3^+$ deletion. From cells cultivated in low-glucose medium for 4 h, during which expression of the integrated $ght5$-GFP gene was induced, Ght5 protein was immunoprecipitated using an anti-GFP monoclonal antibody, and probed in immunoblots using an anti-mono-ubiquitin antibody (see Materials and Methods for details). The anti-ubiquitin antibody produced many bands, most of which were detectable only in immunoprecipitated samples from cells expressing Ght5-GFP, implying that Ght5 is mono-ubiquitylated at multiple positions (top panel, Fig. 6A; Fig. S3B,C). Among these bands, a band with a molecular weight of 110 kDa was clearly detectable in TORC2-deficient $gad8^{ts}$, $tor1Δ$, and $gad8Δ$ mutant cells, but only faintly detected in wild-type cells (indicated by an arrow). Consistently, a band was detected at the corresponding position (indicated by arrowheads) in the α-GFP blot (middle and bottom panels, Fig. 6A). Importantly, this band was nearly absent in $gad8^{ts}$ cells lacking $aly3^+$ ($gad8^{ts}$ $aly3Δ$), indicating that this band represented the Ght5 protein ubiquitylated in an Aly3-dependent manner. To determine the amount of this Aly3-dependent ubiquitylation product of Ght5 in wild-type and mutant cells, the intensity of the 110-kDa band was measured and normalized against that of the total amount of Ght5-GFP protein, which was determined by immunoblotting using the anti-GFP antibody. The ubiquitylated Ght5 was 1.9-fold, 4.4-fold, 3.3-fold and 0.4-fold more abundant in $gad8^{ts}$, $tor1Δ$, $gad8Δ$, and $gad8^{ts}$ $aly3Δ$ mutant cells, respectively, than in wild-type cells (Fig. 6B). Altogether, we concluded that Aly3-dependent ubiquitylation of Ght5, which is believed to be essential for sorting to vacuoles by ESCRT on MVB, is regulated via the TORC2-Gad8 signaling pathway according to extracellular nitrogen level. With nitrogen replenished, TORC2-Gad8 may inhibit Aly3-dependent ubiquitylation of Ght5 so as to prevent Ght5 from being sorted to vacuoles by ESCRT. Upon nitrogen starvation, TORC2 signaling activity may somehow be downregulated, and Ght5 is evidently subjected to Aly3-dependent ubiquitylation. Ubiquitylated Ght5 would be consequently endocytosed to vacuoles to undergo proteolysis.

DISCUSSION

TORC2 signaling is essential for the proper localization of Ght5 glucose/hexose transporters on the cell surface in *S. pombe*. In this report, we reveal how TORC2 signaling ensures the localization of Ght5. TORC2 inhibits Aly3-dependent conjugation of ubiquitin, a recognized molecular tag for the sorting of Ght5 to vacuoles by ESCRT on the endosome/MVB. In wild-type cells, Ght5 was translocated from the surface to vacuoles upon depletion of ammonium ion, and Aly3 was required for this translocation. Signaling by Aly3 α-arrestin and TORC2 may regulate the maintenance of intracellular hexose and amino acid storage by regulating endocytosis and subsequent proteolysis of the Ght5 transporter in response to alterations in nutritional status.

In the budding yeast, *S. cerevisiae*, endocytosis of hexose transporters to vacuoles is triggered by alterations in the concentration of glucose. Glucose limitation in medium results in the activation of AMPK Snf1, which phosphorylates and downregulates the α-arrestin Rod1 so that endocytosis of the hexose transporter Hxt6 to vacuoles is inhibited (Llopis-Torregrosa et al., 2016). In *S. pombe*, although AMPK is essential for cellular adaptation to glucose-limited environments, as in budding yeast,

AMPK is unlikely to be the primary regulator of hexose transporter endocytosis. *S. pombe* AMPK Ssp2 and CAMKK Ssp1, which phosphorylates and activates Ssp2, enhanced transcription of *ght5*[+] upon glucose limitation (Saitoh et al., 2015). Even in TORC2-deficient mutant cells, the level of *ght5* mRNA was elevated to an extent comparable with wild-type cells upon glucose limitation, indicating that AMPK was active enough to promote *ght5*[+] transcription in mutant cells, but not able to block Aly3- and ESCRT-dependent endocytosis of Ght5 to vacuoles. Instead, in *S. pombe*, TORC2 and Gad8 kinases appear to be the primary regulators blocking Aly3-dependent endocytosis of Ght5. Intriguingly, a mammalian α-arrestin, TXNIP, which binds to hexose transporter proteins (GLUT1, GLUT2, GLUT3 and GLUT4) and the ubiquitin ligase, Itch, was reportedly phosphorylated and downregulated via Akt kinase, as well as the AMPK cascade (Waldhart et al., 2017; Wu et al., 2013; Zhang et al., 2010). In human cultured cells, glucose starvation leads to AMPK-dependent phosphorylation of TXNIP (Wu et al., 2013), whereas stimulation with growth factors, including insulin, leads to phosphorylation by Akt kinase, which functions downstream of TORC2 and is orthologous to *S. pombe* Gad8 (Ikeda et al., 2008; Sarbassov et al., 2005; Waldhart et al., 2017). Akt and AMPK phosphorylate the same residue of TXNIP. This phosphorylation attenuates the physical interaction of TXNIP with GLUT transporters, and consequently enables acute glucose uptake (Waldhart et al., 2017), presumably by inhibiting ubiquitylation that results in internalization of GLUT transporters. Thus, phosphorylation of α-arrestin protein via the TORC2 pathway is an evolutionarily conserved mechanism ensuring localization of hexose transporters on the cell surface.

In sharp contrast to budding yeast, in which endocytosis of high-affinity hexose transporters to vacuoles is triggered by the replenishment of glucose (Llopis-Torregrosa et al., 2016), neither glucose depletion nor repletion caused translocation of the high-affinity hexose transporter Ght5 to vacuoles in fission yeast (Fig. 4), although it affected levels of Ght5 protein and mRNA (Saitoh et al., 2015). Translocation of Ght5 to vacuoles was initiated upon depletion of nitrogen, which likely causes amino acid starvation, in fission yeast. Release of Ght5 transporter proteins from the plasma membrane may provide a niche for amino acid transporters, such as Aat1, which localizes on the plasma membrane upon nitrogen starvation (Nakase et al., 2012). Ght5 transported to vacuoles may be subject to proteolysis, which replenishes intracellular amino acid stores. TORC1 is critical for coping with nutritional stress. Upon amino acid starvation, TORC1 becomes inactive so that amino acids are regenerated by autophagy, which is downregulated via the TORC1 signaling pathway under amino acid-rich conditions (Noda and Ohsumi, 1998). Considering our findings and results reported previously (Kawai et al., 2001; Weisman and Choder, 2001), the TORC2 signaling pathway is also important for cellular responses to amino acid starvation.

The findings discussed above raise the question of how the activity of TORC2 kinase is regulated according to nutritional status. Mechanisms controlling TORC1 activity have begun to be uncovered (Bonfils et al., 2012; Chantranupong et al., 2016; Han et al., 2012; Kamada, 2017; Otsubo et al., 2018; Shimobayashi and Hall, 2016; Wolfson et al., 2017). In contrast, it remains unclear how the activity of TORC2 and Gad8 kinases is regulated in response to nutritional changes. As Aly3-dependent endocytosis of Ght5 becomes active under nitrogen starvation, the activities of these kinases were predicted to decrease under such conditions. However, the removal of NH₄Cl from EMM medium containing 111 mM glucose did not affect TORC2 activity, which was measured as the level of Gad8 phosphorylated at Ser^{546} (Hatano et al., 2015). Similarly, although the removal of glucose from nitrogen-rich medium caused a transient reduction of TORC2 signaling, the activity recovered within 30 min to the original level before glucose removal (Hatano et al., 2015). Further studies are necessary to understand the relationship between TORC2/Gad8 activity and nutritional conditions. It is also possible that substrate specificities, as well as the total activities of these kinases, are affected by nitrogen and hexose concentrations. To clarify these points, it will be necessary to examine the phosphorylation status of Aly3 under various conditions, as it is likely to be a substrate of Gad8 kinase (see below); therefore, its phosphorylation level may reflect Gad8 activity *in vivo*.

As mentioned above, human TXNIP is reportedly phosphorylated by Akt, the human equivalent of Gad8, at Ser308 (Waldhart et al., 2017). Although the amino acid sequence around this serine is not conserved between Aly3 and TXNIP (Fig. 3B), Aly3 harbors Ser460, which matches a consensus sequence for Akt substrates (Arg-x-Arg-x-x-Ser/Thr, where 'x' denotes any amino acid; Manning and Cantley, 2007), and Ser460 was indeed phosphorylated (Kettenbach et al., 2015). Therefore, we suspect that *S. pombe* Aly3 is phosphorylated directly by Gad8/Akt at Ser460, and that as in TXNIP, this phosphorylation may attenuate physical interactions between Aly3 and Ght5.

As in many other α-arrestin proteins, Aly3 contains two proline-rich PY motifs, a typical consensus sequence of which is Pro/Leu/Val-Pro-x-Tyr (Becuwe et al., 2012a; Chen et al., 1997; Chen and Sudol, 1995), in the C-terminal region (508-511 and 526-529, Fig. 3B). In budding yeast, PY motifs of Rod1 α-arrestin interact with the WW domain of the Nedd4-like ubiquitin ligase, Rsp5 (Andoh et al., 2002; Becuwe et al., 2012b). Likewise, in humans, TXNIP α-arrestin interacts with ITCH ubiquitin ligase via its PY motifs and WW domains (Zhang et al., 2010). Although the ubiquitin ligase binding site on Aly3 remains to be identified, we suspect that a Nedd4-like ubiquitin ligase containing a WW domain, encoded by three genes in the *S. pombe* genome (*pub1*[+], *pub2*[+] and *pub3*[+], Lock et al., 2019), may bind to Aly3 and ubiquitylate Ght5 for vacuolar transport. It is noteworthy that GFP-fused Pub1 localizes on the Golgi, as well as the cell surface, whereas Pub2-GFP and Pub3-GFP localize predominantly on the cell surface (Matsuyama et al., 2006; Tamai and Shimoda, 2002). Pub1 interacts with the β-arrestin Any1, and this Pub1-Any1 complex ubiquitylates the amino acid transporter Aat1. Ubiquitylated Aat1 is confined to the Golgi, and is not transported to the cell surface under nitrogen-rich conditions (Nakase et al., 2012, 2013). Thus, Pub2 and/or Pub3 may interact with α-arrestin and ubiquitylate cell surface proteins, including Ght5, whereas Pub1-interacting β-arrestin may ubiquitylate substrates in the Golgi.

In suppressor screening performed in this study, TORC1-related mutations were identified in addition to mutations in genes encoding Aly3 α-arrestin and ESCRT proteins. Loss-of-function mutations in *tsc1*[+], *tsc2*[+], *gtr1*[+], *npr2*[+] and *tip41*[+] restored the proper localization of Ght5 on the surface of *gad8*[ts] mutant cells defective in the TORC2 signaling pathway. Based on earlier studies, these gene products appear to function as negative regulators of TORC1 kinase activity in fission yeast (Chia et al., 2017; Fenyvuesvolgyi et al., 2005; Fukuda and Shiozaki, 2018; Inoki et al., 2002; Jacinto et al., 2001; Manning and Cantley, 2003; Saxton and Sabatini, 2017; Tee et al., 2003). Thus, loss-of-function mutations in these genes supposedly result in ectopic activation of TORC1. Although it remains unclear why ectopic activation of TORC1 restores proper localization of Ght5 in TORC2-deficient
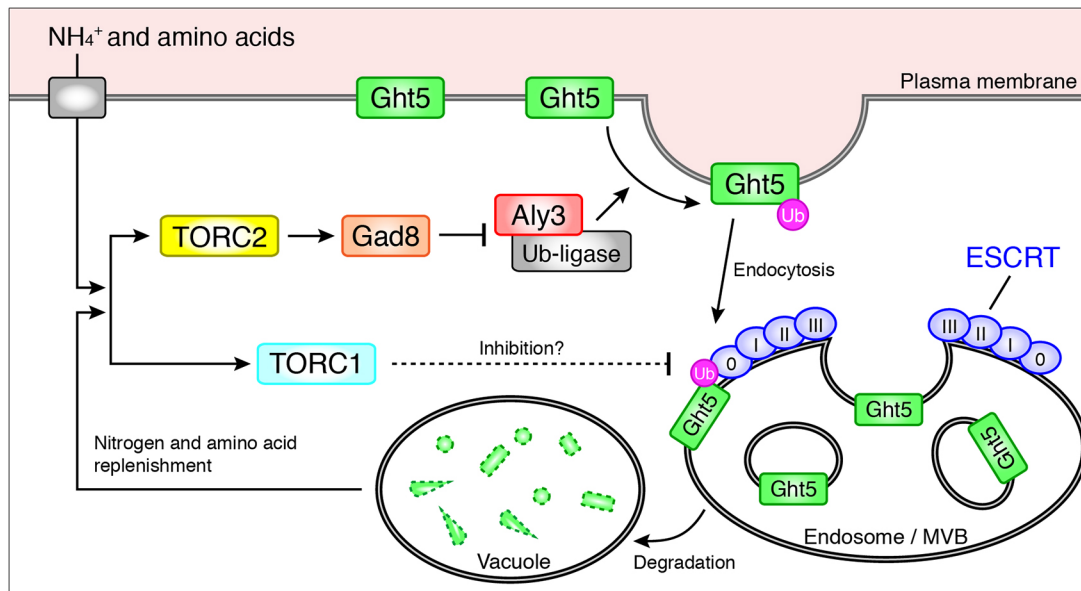
Fig. 7. A schematic model of how the TORC2 signaling pathway regulates Aly3-dependent vacuolar transport of Ght5 in *S. pombe*. In wild-type cells under nitrogen-rich conditions, the TORC2-Gad8 signaling pathway inhibits Aly3-dependent ubiquitylation of Ght5, so that Ght5 is hypo-ubiquitylated and localized on the cell surface regardless of the presence or absence of Aly3. In nitrogen-starved wild-type cells, as well as mutant cells defective in the TORC2-Gad8 signaling pathway, Ght5 undergoes Aly3-dependent ubiquitylation, is captured by the ESCRT machinery (blue circles) and is eventually transported to a vacuole for protein degradation. Replenishment of nitrogen and amino acids may activate the TORC1 and the TORC2-Gad8 signaling pathways, and activated TORC1 may negatively regulate the ESCRT machinery. See main text for details.

cells, we suspect that TORC1 may also regulate the ESCRT function in a manner different from that of TORC2 (Fig. 7). TORC1 reportedly negatively regulates the formation of the ESCRT-0 complex on the vacuolar membrane, which is required for micro-autophagy (Morshed et al., 2020). Thus, likewise, ectopically activated TORC1 may inhibit ESCRT-0 complex formation on endosomal membranes, which is required for endocytosis of Ght5 from the cell surface to vacuoles.

In summary, we discovered the mechanism that ensures the proper localization of the high-affinity glucose/hexose transporter Ght5 on the cell surface via the TORC2-Gad8 signaling pathway. TORC2-Gad8 inhibits Aly3-dependent ubiquitylation of Ght5, which causes its translocation from the surface to vacuoles in an ESCRT-dependent manner, in nitrogen-replenished medium. Although TORC2 has not been shown to regulate hexose transporter endocytosis in other yeasts, trafficking of mammalian GLUT hexose transporters from the surface to the cytosol was recently shown to be regulated similarly by the TXNIP α-arrestin and Gad8-related Akt upon insulin stimulation. Therefore, this study offers new insights into evolutionarily conserved molecular mechanisms to control intracellular localization of hexose transporters responding to nutritional/growth hormone stimuli.

MATERIALS AND METHODS
Strains and general techniques
The culture medium used for fission yeast cultivation were yeast extract with supplements (YES, rich medium) and EMM2 (minimal medium) (Moreno et al., 1991), with modified concentrations of glucose and/or ammonium chloride, as indicated. Unless otherwise stated, wild-type and *aly3Δ* cells were cultivated at 33°C, whereas strains harboring a *gad8*[ts] (S240P) mutation, *gad8Δ* mutant and *tor1Δ* mutant were cultivated at 26°C. The *S. pombe* strain expressing Ght5-GFP was reported previously (Saitoh et al., 2015). For gene disruption, a PCR-mediated method was used (Krawchuk and Wahls, 1999). Gene deletion in each strain was confirmed by PCR. Sequences of the primers used for gene deletion are listed in Table S1. Cell

viability was expressed as the ratio of the number of colonies formed on YES solid medium, containing 167 mM (3%) glucose, to the total number (~1000) of cell bodies plated, after 3 days incubation at 30°C. Amino acid sequences were aligned using Clustal Omega (Sievers et al., 2011).

Suppressor screening and whole-genome sequencing
To identify suppressor mutations that restored the proliferation defect of the *gad8*[ts] mutant in low glucose, 10^7 *gad8*[ts] mutant cells were cultivated on solid YES medium containing 3.3 mM (0.06%) glucose, at a concentration of $1×10^6$ cells per plate, at 33°C, obtaining 370 colonies after 6 days. Out of 370 strains, 49 strains were selected for whole-genome sequencing, as they were confirmed to proliferate on solid YES medium containing 0.06% glucose better than the original *gad8*[ts] strain. From the original *gad8*[ts] mutant and the 49 revertant strains, genomic DNA was gently extracted essentially as reported previously (Murray et al., 2016), and then purified with AMPure XP (Beckman Coulter, Brea, CA, USA). Sequencing libraries were prepared using a TruSeq DNA PCR-Free kit (Illumina, San Diego, CA, USA) according to the manufacturer's instructions. Cluster amplification and 151-bp paired-end sequencing were performed according to the manufacturer's protocol for NovaSeq 6000 (Illumina).

Sequencing data analysis
The quality of raw sequence data was analyzed using FastQC 0.11.8 (www.bioinformatics.babraham.ac.uk/projects/fastqc/). All reads were mapped to the *S. pombe* reference genome using BWA 0.7.17 (Li and Durbin, 2009), followed by variant calls using samtools 1.9 and bcftools 1.9 (Li, 2011; Li et al., 2009). Unique mutations, which were found in revertant strains, but not in the original *gad8*[ts] strain, were extracted using bcftools. Unique mutations listed in Table 1 were annotated using SnpEff 4.3.1 (Cingolani et al., 2012).

Light microscopy and image analysis
Fluorescence microscopy was performed using an Olympus IX81 microscope (Olympus, Tokyo, Japan) equipped with a 100× objective lens (numerical aperture 1.40) and a charge-coupled device camera, or a confocal microscope (Digital Eclipse C1; Nikon, Tokyo, Japan) equipped with a 100× objective lens (NA 1.49). To image live cells, the cell culture was concentrated by brief centrifugation, and the sample was kept on ice

until imaging. To stain vacuoles, cells were cultivated in EMM2 containing 4.4 mM (0.08%) glucose supplemented with 16 µM FM4-64 (Thermo Fisher Scientific, Waltham, MA, USA) for 30 min in the dark. Cells were then washed twice in fresh low-glucose EMM2 without FM4-64, and cultured for 30 min before imaging. The brightness and contrast of the acquired images were adjusted using ImageJ software (National Institutes of Health, Bethesda, MD, USA).

Total RNA preparation and RT-qPCR

Total RNA was prepared from fission yeast cells using the hot phenol extraction method (Lyne et al., 2003). cDNA was synthesized using a ReverTra Ace qPCR RT Kit (Toyobo, Osaka, Japan). qPCR was performed using a LightCycler system (Roche, Basel, Switzerland) and a FastStart Essential DNA Green Master Mix (Roche). The $aly3^+$ mRNA level relative to $act1^+$ was calculated using a standard curve drawn using serial dilutions of genomic DNA containing the same number of DNA fragments of $aly3^+$ and $act1^+$ as a template. PCR primer sequences for $aly3^+$ were as follows: 5′-CGTAGCGCATGTACCCTTAAT-3′ and 5′-ATCAAGCGGCAAGAC-ATTAGTA-3′.

Immunoprecipitation, immunoblotting and image quantification

For affinity-purification of Ght5-GFP, cells were collected after 4 h of cultivation in EMM2 containing 4.4 mM glucose at 33°C. They were washed once in cold wash buffer [50 mM Tris-HCl (pH 7.5), 150 mM NaCl, 5 mM NaF and 1 mM PMSF], and stored at −80°C until use. Protein extracts were prepared by vortexing the cells with glass beads in cold lysis buffer [50 mM Tris-HCl (pH 7.5), 150 mM NaCl, 5 mM EDTA, 10% glycerol, 20 mM β-glycerophosphate, 10 mM p-nitrophenyl phosphate, 10 mM NaF, 0.1 mM sodium orthovanadate (Na_3VO_4), 1 mM dithiothreitol (DTT), 0.5% Nonidet P-40, 10 µM MG-132 (Calbiochem, Darmstadt, Germany), 10 µM ubiquitin isopeptidase inhibitor I G5 (G5, Calbiochem), protease inhibitor cocktail (Nacalai Tesque, Kyoto, Japan) and 2 mM PMSF]. Crude lysate was centrifuged at 17,700 g for 15 min at 4°C in a microcentrifuge (Kitman-24, Tomy Seiko, Tokyo, Japan) to prepare input protein extracts for immunoprecipitation. The total protein concentration of each sample was determined using a Protein Assay Dye Reagent (#500-0006, Bio-Rad, Richmond, CA) with an optical density reading at 595 nm (OD_{595}). Input protein extracts with an OD_{595}=30 were mixed with anti-GFP antibody-conjugated agarose beads (#06083-05, Nacalai Tesque) that had been washed in bead wash buffer [10 mM Tris-HCl (pH 7.5), 150 mM NaCl and 0.5 mM EDTA]. The mixture was incubated on a rotating mixer for 2 h at 4°C. Beads were washed 3× in immunoprecipitation wash buffer [50 mM Tris-HCl (pH 7.5), 150 mM NaCl, 5 mM EDTA, 10% glycerol, 2 mM β-glycerophosphate, 1 mM p-nitrophenyl phosphate, 1 mM NaF, 0.01 mM Na_3VO_4, 0.1 mM DTT, 0.05% Nonidet P-40, 1 µM MG-132, 1 µM G5, protease inhibitor cocktail and 0.1 mM PMSF]. To separate proteins by SDS-PAGE, the input extract and washed beads were mixed with lithium dodecyl sulfate (LDS) sample buffer [0.25 M Tris-HCl (pH 8.5), 10% glycerol, 0.5 mM EDTA, 2% LDS, 2.5% β-mercaptoethanol and a trace amount of bromophenol blue] and incubated on ice for 2 h. Immunoprecipitates derived from cell lysates of OD_{595}=10 and washed beads ('beads only' in Fig. 6A and Fig. S3B) were separated by SDS-PAGE. To detect Ght5-GFP in crude lysates, samples were prepared as reported previously (Saitoh et al., 2015).

Immunoblotting was performed essentially as described previously (Toyoda et al., 2018). Primary antibodies used were anti-GFP (1:20,000, rabbit, ab32146, Abcam, Cambridge, UK), anti-ubiquitin (1:200, mouse, clone 1B3, MK-11-3, MBL, Nagoya, Japan) and anti-PSTAIR (1:3000, mouse, P7962, Merck, Darmstadt, Germany) antibodies. For secondary antibodies, CF680- or CF770-conjugated anti-mouse and anti-rabbit IgG antibodies (1:5000, #20067 and #20077, Biotium, Hayward, CA, USA) were used. Antibodies were diluted in Blocking One (Nacalai Tesque). Nitrocellulose membranes were washed in Tris-buffered saline containing 0.1% Tween-20 (Nacalai Tesque). Fluorescence on membranes was detected using an Odyssey instrument (LI-COR, Lincoln, NE, USA). Fluorescence intensities were analyzed using ImageStudioLite software (LI-COR). To quantify the ubiquitylated form of Ght5-GFP (Ub-Ght5-GFP) in the immunoprecipitated fraction, background intensity at 200 kDa for each lane was subtracted from that of the 110-kDa band. Then, the intensity of Ub-Ght5-GFP was divided by that of the total Ght5-GFP in the immunoprecipitated fraction to obtain the signal intensity ratio of Ub-Ght5-GFP to total Ght5-GFP.

References

Alessi, D. R., James, S. R., Downes, C. P., Holmes, A. B., Gaffney, P. R., Reese, C. B. and Cohen, P. (1997). Characterization of a 3-phosphoinositide-dependent protein kinase which phosphorylates and activates protein kinase Balpha. *Curr. Biol.* **7**, 261-269. doi:10.1016/S0960-9822(06)00122-9

Alvarez, C. E. (2008). On the origins of arrestin and rhodopsin. *BMC Evol. Biol.* **8**, 222. doi:10.1186/1471-2148-8-222

Andoh, T., Hirata, Y. and Kikuchi, A. (2002). PY motifs of Rod1 are required for binding to Rsp5 and for drug resistance. *FEBS Lett.* **525**, 131-134. doi:10.1016/S0014-5793(02)03104-6

Antonescu, C. N., McGraw, T. E. and Klip, A. (2014). Reciprocal regulation of endocytosis and metabolism. *Cold Spring Harb. Perspect Biol.* **6**, a016964. doi:10.1101/cshperspect.a016964

Bar-Peled, L., Schweitzer, L. D., Zoncu, R. and Sabatini, D. M. (2012). Ragulator is a GEF for the rag GTPases that signal amino acid levels to mTORC1. *Cell* **150**, 1196-1208. doi:10.1016/j.cell.2012.07.032

Bar-Peled, L., Chantranupong, L., Cherniack, A. D., Chen, W. W., Ottina, K. A., Grabiner, B. C., Spear, E. D., Carter, S. L., Meyerson, M. and Sabatini, D. M. (2013). A Tumor suppressor complex with GAP activity for the Rag GTPases that signal amino acid sufficiency to mTORC1. *Science* **340**, 1100-1106. doi:10.1126/science.1232044

Barbet, N. C., Schneider, U., Helliwell, S. B., Stansfield, I., Tuite, M. F. and Hall, M. N. (1996). TOR controls translation initiation and early G1 progression in yeast. *Mol. Biol. Cell* **7**, 25-42. doi:10.1091/mbc.7.1.25

Becuwe, M., Herrador, A., Haguenauer-Tsapis, R., Vincent, O. and Léon, S. (2012a). Ubiquitin-mediated regulation of endocytosis by proteins of the arrestin family. *Biochem. Res. Int.* **2012**, 242764. doi:10.1155/2012/242764

Becuwe, M., Vieira, N., Lara, D., Gomes-Rezende, J., Soares-Cunha, C., Casal, M., Haguenauer-Tsapis, R., Vincent, O., Paiva, S. and Léon, S. (2012b). A molecular switch on an arrestin-like protein relays glucose signaling to transporter endocytosis. *J. Cell Biol.* **196**, 247-259. doi:10.1083/jcb.201109113

Bonfils, G., Jaquenoud, M., Bontron, S., Ostrowicz, C., Ungermann, C. and De Virgilio, C. (2012). Leucyl-tRNA synthetase controls TORC1 via the EGO complex. *Mol. Cell* **46**, 105-110. doi:10.1016/j.molcel.2012.02.009

Chantranupong, L., Scaria, S. M., Saxton, R. A., Gygi, M. P., Shen, K., Wyant, G. A., Wang, T., Harper, J. W., Gygi, S. P. and Sabatini, D. M. (2016). The CASTOR proteins are arginine sensors for the mTORC1 pathway. *Cell* **165**, 153-164. doi:10.1016/j.cell.2016.02.035

Chen, H. I. and Sudol, M. (1995). The WW domain of Yes-associated protein binds a proline-rich ligand that differs from the consensus established for Src homology 3-binding modules. *Proc. Natl. Acad. Sci. USA* **92**, 7819-7823. doi:10.1073/pnas.92.17.7819

Chen, H. I., Einbond, A., Kwak, S. J., Linn, H., Koepf, E., Peterson, S., Kelly, J. W. and Sudol, M. (1997). Characterization of the WW domain of human yes-associated protein and its polyproline-containing ligands. J. Biol. Chem. 272, 17070-17077. doi:10.1074/jbc.272.27.17070

Chia, K. H., Fukuda, T., Sofyantoro, F., Matsuda, T., Amai, T. and Shiozaki, K. (2017). Ragulator and GATOR1 complexes promote fission yeast growth by attenuating TOR complex 1 through Rag GTPases. Elife 6, e30880. doi:10.7554/eLife.30880.024

Cingolani, P., Platts, A., Wang le, L., Coon, M., Nguyen, T., Wang, L., Land, S. J., Lu, X. and Ruden, D. M. (2012). A program for annotating and predicting the effects of single nucleotide polymorphisms, SnpEff: SNPs in the genome of Drosophila melanogaster strain w1118; iso-2; iso-3. Fly (Austin) 6, 80-92. doi:10.4161/fly.19695

Clague, M. J., Liu, H. and Urbé, S. (2012). Governance of endocytic trafficking and signaling by reversible ubiquitylation. Dev. Cell 23, 457-467. doi:10.1016/j.devcel.2012.08.011

Dudin, O., Merlini, L., Bendezú, F. O., Groux, R., Vincenzetti, V. and Martin, S. G. (2017). A systematic screen for morphological abnormalities during fission yeast sexual reproduction identifies a mechanism of actin aster formation for cell fusion. PLoS Genet. 13, e1006721. doi:10.1371/journal.pgen.1006721

Fenyvuesvolgyi, C., Elder, R. T., Benko, Z., Liang, D. and Zhao, R. Y. (2005). Fission yeast homologue of Tip41-like proteins regulates type 2A phosphatases and responses to nitrogen sources. Biochim. Biophys. Acta 1746, 155-162. doi:10.1016/j.bbamcr.2005.09.006

Fukuda, T. and Shiozaki, K. (2018). The Rag GTPase-Ragulator complex attenuates TOR complex 1 signaling in fission yeast. Autophagy 14, 1105-1106. doi:10.1080/15548627.2018.1444313

Han, J. M., Jeong, S. J., Park, M. C., Kim, G., Kwon, N. H., Kim, H. K., Ha, S. H., Ryu, S. H. and Kim, S. (2012). Leucyl-tRNA synthetase is an intracellular leucine sensor for the mTORC1-signaling pathway. Cell 149, 410-424. doi:10.1016/j.cell.2012.02.044

Hatano, T., Morigasaki, S., Tatebe, H., Ikeda, K. and Shiozaki, K. (2015). Fission yeast Ryh1 GTPase activates TOR Complex 2 in response to glucose. Cell Cycle 14, 848-856. doi:10.1080/15384101.2014.1000215

Hayashi, T., Hatanaka, M., Nagao, K., Nakaseko, Y., Kanoh, J., Kokubu, A., Ebe, M. and Yanagida, M. (2007). Rapamycin sensitivity of the Schizosaccaromyces pombe tor2 mutant and organization of two highly phosphorylated TOR complexes by specific and common subunits. Genes Cells 12, 1357-1370. doi:10.1111/j.1365-2443.2007.01141.x

Heiland, S., Radovanovic, N., Höfer, M., Winderickx, J. and Lichtenberg, H. (2000). Multiple hexose transporters of Schizosaccharomyces pombe. J. Bacteriol. 182, 2153-2162. doi:10.1128/JB.182.8.2153-2162.2000

Hovsepian, J., Defenouillère, Q., Albanèse, V., Váchová, L., Garcia, C., Palková, Z. and Léon, S. (2017). Multilevel regulation of an α-arrestin by glucose depletion controls hexose transporter endocytosis. J. Cell Biol. 216, 1811-1831. doi:10.1083/jcb.201610094

Hsiao, W.-Y., Wang, Y.-T. and Wang, S.-W. (2020). Fission yeast Puf2, a pumilio and FBF family RNA-binding protein, links stress granules to processing bodies. Mol. Cell. Biol. 40, e00589. doi:10.1128/MCB.00589-19

Ikeda, K., Morigasaki, S., Tatebe, H., Tamanoi, F. and Shiozaki, K. (2008). Fission yeast TOR complex 2 activates the AGC-family Gad8 kinase essential for stress resistance and cell cycle control. Cell Cycle 7, 358-364. doi:10.4161/cc.7.3.5245

Inoki, K., Li, Y., Zhu, T., Wu, J. and Guan, K.-L. (2002). TSC2 is phosphorylated and inhibited by Akt and suppresses mTOR signalling. Nat. Cell Biol. 4, 648-657. doi:10.1038/ncb839

Jacinto, E., Guo, B., Arndt, K. T., Schmelzle, T. and Hall, M. N. (2001). TIP41 interacts with TAP42 and negatively regulates the TOR signaling pathway. Mol. Cell 8, 1017-1026. doi:10.1016/S1097-2765(01)00386-0

Kamada, Y. (2017). Novel tRNA function in amino acid sensing of yeast Tor complex1. Genes Cells 22, 135-147. doi:10.1111/gtc.12462

Katzmann, D. J., Babst, M. and Emr, S. D. (2001). Ubiquitin-dependent sorting into the multivesicular body pathway requires the function of a conserved endosomal protein sorting complex, ESCRT-I. Cell 106, 145-155. doi:10.1016/S0092-8674(01)00434-2

Kawai, M., Nakashima, A., Ueno, M., Ushimaru, T., Aiba, K., Doi, H. and Uritani, M. (2001). Fission yeast tor1 functions in response to various stresses including nitrogen starvation, high osmolarity, and high temperature. Curr. Genet. 39, 166-174. doi:10.1007/s002940100198

Kettenbach, A. N., Deng, L., Wu, Y., Baldissard, S., Adamo, M. E., Gerber, S. A. and Moseley, J. B. (2015). Quantitative phosphoproteomics reveals pathways for coordination of cell growth and division by the conserved fission yeast kinase pom1. Mol. Cell. Proteomics 14, 1275-1287. doi:10.1074/mcp.M114.045245

Krawchuk, M. D. and Wahls, W. P. (1999). High-efficiency gene targeting in Schizosaccharomyces pombe using a modular, PCR-based approach with long tracts of flanking homology. Yeast 15, 1419-1427. doi:10.1002/(SICI)1097-0061(19990930)15:13<1419::AID-YEA466>3.0.CO;2-Q

Li, H. (2011). A statistical framework for SNP calling, mutation discovery, association mapping and population genetical parameter estimation from sequencing data. Bioinformatics 27, 2987-2993. doi:10.1093/bioinformatics/btr509

Li, H. and Durbin, R. (2009). Fast and accurate short read alignment with Burrows-Wheeler transform. Bioinformatics 25, 1754-1760. doi:10.1093/bioinformatics/btp324

Li, H., Handsaker, B., Wysoker, A., Fennell, T., Ruan, J., Homer, N., Marth, G., Abecasis, G. and Durbin, R. (2009). The sequence alignment/map format and SAMtools. Bioinformatics 25, 2078-2079. doi:10.1093/bioinformatics/btp352

Llopis-Torregrosa, V., Ferri-Blázquez, A., Adam-Artigues, A., Deffontaines, E., van Heusden, G. P. and Yenush, L. (2016). Regulation of the yeast Hxt6 hexose transporter by the Rod1 α-arrestin, the Snf1 protein kinase, and the Bmh2 14-3-3 Protein. J. Biol. Chem. 291, 14973-14985. doi:10.1074/jbc.M116.733923

Lock, A., Rutherford, K., Harris, M. A., Hayles, J., Oliver, S. G., Bähler, J. and Wood, V. (2019). PomBase 2018: user-driven reimplementation of the fission yeast database provides rapid and intuitive access to diverse, interconnected information. Nucleic Acids Res. 47, D821-d827. doi:10.1093/nar/gky961

Long, X., Lin, Y., Ortiz-Vega, S., Yonezawa, K. and Avruch, J. (2005). Rheb binds and regulates the mTOR kinase. Curr. Biol. 15, 702-713. doi:10.1016/j.cub.2005.02.053

Lyne, R., Burns, G., Mata, J., Penkett, C. J., Rustici, G., Chen, D., Langford, C., Vetrie, D. and Bahler, J. (2003). Whole-genome microarrays of fission yeast: characteristics, accuracy, reproducibility, and processing of array data. BMC Genomics 4, 27. doi:10.1186/1471-2164-4-27

Manning, B. D. and Cantley, L. C. (2003). Rheb fills a GAP between TSC and TOR. Trends Biochem. Sci. 28, 573-576. doi:10.1016/j.tibs.2003.09.003

Manning, B. D. and Cantley, L. C. (2007). AKT/PKB signaling: navigating downstream. Cell 129, 1261-1274. doi:10.1016/j.cell.2007.06.009

Matsuyama, A., Arai, R., Yashiroda, Y., Shirai, A., Kamata, A., Sekido, S., Kobayashi, Y., Hashimoto, A., Hamamoto, M., Hiraoka, Y. et al. (2006). ORFeome cloning and global analysis of protein localization in the fission yeast Schizosaccharomyces pombe. Nat. Biotechnol. 24, 841-847. doi:10.1038/nbt1222

Mitchell, A. L., Attwood, T. K., Babbitt, P. C., Blum, M., Bork, P., Bridge, A., Brown, S. D., Chang, H. Y., El-Gebali, S., Fraser, M. I. et al. (2019). InterPro in 2019: improving coverage, classification and access to protein sequence annotations. Nucleic Acids Res. 47, D351-d360. doi:10.1093/nar/gky1100

Moreno, S., Klar, A. and Nurse, P. (1991). Molecular genetic analysis of fission yeast Schizosaccharomyces pombe. Methods Enzymol. 194, 795-823. doi:10.1016/0076-6879(91)94059-L

Morshed, S., Sharmin, T. and Ushimaru, T. (2020). TORC1 regulates ESCRT-0 complex formation on the vacuolar membrane and microautophagy induction in yeast. Biochem. Biophys. Res. Commun. 522, 88-94. doi:10.1016/j.bbrc.2019.11.064

Mukaiyama, H., Kajiwara, S., Hosomi, A., Giga-Hama, Y., Tanaka, N., Nakamura, T. and Takegawa, K. (2009). Autophagy-deficient Schizosaccharomyces pombe mutants undergo partial sporulation during nitrogen starvation. Microbiology (Read.) 155, 3816-3826. doi:10.1099/mic.0.034389-0

Murray, J. M., Watson, A. T. and Carr, A. M. (2016). Extraction of Chromosomal DNA from Schizosaccharomyces pombe. Cold Spring Harb. Protoc. 2016, 484-487. doi:10.1101/pdb.prot090985

Nakase, M., Nakase, Y., Chardwiriyapreecha, S., Kakinuma, Y., Matsumoto, T. and Takegawa, K. (2012). Intracellular trafficking and ubiquitination of the Schizosaccharomyces pombe amino acid permease Aat1p. Microbiology (Read.) 158, 659-673. doi:10.1099/mic.0.053389-0

Nakase, Y., Nakase, M., Kashiwazaki, J., Murai, T., Otsubo, Y., Mabuchi, I., Yamamoto, M., Takegawa, K. and Matsumoto, T. (2013). The fission yeast β-arrestin-like protein Any1 is involved in TSC-Rheb signaling and the regulation of amino acid transporters. J. Cell Sci. 126, 3972-3981. doi:10.1242/jcs.128355

Niederberger, C. and Schweingruber, M. E. (1999). A Schizosaccharomyces pombe gene, ksg1, that shows structural homology to the human phosphoinositide-dependent protein kinase PDK1, is essential for growth, mating and sporulation. Mol. Gen. Genet. 261, 177-183. doi:10.1007/s004380050955

Nikko, E. and Pelham, H. R. (2009). Arrestin-mediated endocytosis of yeast plasma membrane transporters. Traffic 10, 1856-1867. doi:10.1111/j.1600-0854.2009.00990.x

Noda, T. and Ohsumi, Y. (1998). Tor, a phosphatidylinositol kinase homologue, controls autophagy in yeast. J. Biol. Chem. 273, 3963-3966. doi:10.1074/jbc.273.7.3963

O'Donnell, A. F. and Schmidt, M. C. (2019). AMPK-mediated regulation of alpha-arrestins and protein trafficking. Int. J. Mol. Sci. 20, 515-534. doi:10.3390/ijms20030515

O'Donnell, A. F., McCartney, R. R., Chandrashekarappa, D. G., Zhang, B. B., Thorner, J. and Schmidt, M. C. (2015). 2-Deoxyglucose impairs Saccharomyces cerevisiae growth by stimulating Snf1-regulated and α-arrestin-mediated trafficking of hexose transporters 1 and 3. Mol. Cell. Biol. 35, 939-955. doi:10.1128/MCB.01183-14

Otsubo, Y., Matsuo, T., Nishimura, A., Yamamoto, M. and Yamashita, A. (2018). tRNA production links nutrient conditions to the onset of sexual differentiation through the TORC1 pathway. EMBO Rep. 19, e44867. doi:10.15252/embr.201744867

Powers, T. and Walter, P. (1999). Regulation of ribosome biogenesis by the rapamycin-sensitive TOR-signaling pathway in Saccharomyces cerevisiae. *Mol. Biol. Cell* **10**, 987-1000. doi:10.1091/mbc.10.4.987

Puca, L. and Brou, C. (2014). Α-arrestins - new players in Notch and GPCR signaling pathways in mammals. *J. Cell Sci.* **127**, 1359-1367. doi:10.1242/jcs.142539

Roy, A., Kim, Y.-B., Cho, K. H. and Kim, J.-H. (2014). Glucose starvation-induced turnover of the yeast glucose transporter Hxt1. *Biochim. Biophys. Acta* **1840**, 2878-2885. doi:10.1016/j.bbagen.2014.05.004

Saitoh, S., Mori, A., Uehara, L., Masuda, F., Soejima, S. and Yanagida, M. (2015). Mechanisms of expression and translocation of major fission yeast glucose transporters regulated by CaMKK/phosphatases, nuclear shuttling, and TOR. *Mol. Biol. Cell* **26**, 373-386. doi:10.1091/mbc.E14-11-1503

Sancak, Y., Bar-Peled, L., Zoncu, R., Markhard, A. L., Nada, S. and Sabatini, D. M. (2010). Ragulator-Rag complex targets mTORC1 to the lysosomal surface and is necessary for its activation by amino acids. *Cell* **141**, 290-303. doi:10.1016/j.cell.2010.02.024

Sarbassov, D. D., Guertin, D. A., Ali, S. M. and Sabatini, D. M. (2005). Phosphorylation and regulation of Akt/PKB by the rictor-mTOR complex. *Science* **307**, 1098-1101. doi:10.1126/science.1106148

Saxton, R. A. and Sabatini, D. M. (2017). mTOR Signaling in growth, metabolism, and disease. *Cell* **168**, 960-976. doi:10.1016/j.cell.2017.02.004

Shimobayashi, M. and Hall, M. N. (2016). Multiple amino acid sensing inputs to mTORC1. *Cell Res.* **26**, 7-20. doi:10.1038/cr.2015.146

Sievers, F., Wilm, A., Dineen, D., Gibson, T. J., Karplus, K., Li, W., Lopez, R., McWilliam, H., Remmert, M., Söding, J. et al. (2011). Fast, scalable generation of high-quality protein multiple sequence alignments using Clustal Omega. *Mol. Syst. Biol.* **7**, 539. doi:10.1038/msb.2011.75

Sorkin, A. (2000). The endocytosis machinery. *J. Cell Sci.* **113**, 4375-4376.

Stokoe, D., Stephens, L. R., Copeland, T., Gaffney, P. R., Reese, C. B., Painter, G. F., Holmes, A. B., McCormick, F. and Hawkins, P. T. (1997). Dual role of phosphatidylinositol-3,4,5-trisphosphate in the activation of protein kinase B. *Science* **277**, 567-570. doi:10.1126/science.277.5325.567

Takeda, K., Mori, A. and Yanagida, M. (2011). Identification of genes affecting the toxicity of anti-cancer drug bortezomib by genome-wide screening in S. pombe. *PLoS ONE* **6**, e22021. doi:10.1371/journal.pone.0022021

Tamai, K. K. and Shimoda, C. (2002). The novel HECT-type ubiquitin-protein ligase Pub2p shares partially overlapping function with Pub1p in Schizosaccharomyces pombe. *J. Cell Sci.* **115**, 1847-1857.

Tatebe, H. and Shiozaki, K. (2010). Rab small GTPase emerges as a regulator of TOR complex 2. *Small GTPases* **1**, 180-182. doi:10.4161/sgtp.1.3.14936

Tee, A. R., Manning, B. D., Roux, P. P., Cantley, L. C. and Blenis, J. (2003). Tuberous sclerosis complex gene products, Tuberin and Hamartin, control mTOR signaling by acting as a GTPase-activating protein complex toward Rheb. *Curr. Biol.* **13**, 1259-1268. doi:10.1016/S0960-9822(03)00506-2

Toyoda, Y., Akarlar, B., Sarov, M., Ozlu, N. and Saitoh, S. (2018). Extracellular glucose level regulates dependence on GRP78 for cell surface localization of multipass transmembrane proteins in HeLa cells. *FEBS Lett.* **592**, 3295-3304. doi:10.1002/1873-3468.13232

Ukleja, M., Cuellar, J., Siwaszek, A., Kasprzak, J. M., Czarnocki-Cieciura, M., Bujnicki, J. M., Dziembowski, A. and Valpuesta, J. M. (2016). The architecture of the Schizosaccharomyces pombe CCR4-NOT complex. *Nat. Commun.* **7**, 10433. doi:10.1038/ncomms10433

Vietri, M., Radulovic, M. and Stenmark, H. (2020). The many functions of ESCRTs. *Nat. Rev. Mol. Cell Biol.* **21**, 25-42. doi:10.1038/s41580-019-0177-4

Waldhart, A. N., Dykstra, H., Peck, A. S., Boguslawski, E. A., Madaj, Z. B., Wen, J., Veldkamp, K., Hollowell, M., Zheng, B., Cantley, L. C. et al. (2017). Phosphorylation of TXNIP by AKT mediates acute influx of glucose in response to insulin. *Cell Rep* **19**, 2005-2013. doi:10.1016/j.celrep.2017.05.041

Weisman, R. and Choder, M. (2001). The fission yeast TOR homolog, tor1+, is required for the response to starvation and other stresses via a conserved serine. *J. Biol. Chem.* **276**, 7027-7032. doi:10.1074/jbc.M010446200

Wilden, U., Hall, S. W. and Kühn, H. (1986). Phosphodiesterase activation by photoexcited rhodopsin is quenched when rhodopsin is phosphorylated and binds the intrinsic 48-kDa protein of rod outer segments. *Proc. Natl. Acad. Sci. USA* **83**, 1174-1178. doi:10.1073/pnas.83.5.1174

Wolfson, R. L., Chantranupong, L., Wyant, G. A., Gu, X., Orozco, J. M., Shen, K., Condon, K. J., Petri, S., Kedir, J., Scaria, S. M. et al. (2017). KICSTOR recruits GATOR1 to the lysosome and is necessary for nutrients to regulate mTORC1. *Nature* **543**, 438-442. doi:10.1038/nature21423

Wood, V., Gwilliam, R., Rajandream, M. A., Lyne, M., Lyne, R., Stewart, A., Sgouros, J., Peat, N., Hayles, J., Baker, S. et al. (2002). The genome sequence of Schizosaccharomyces pombe. *Nature* **415**, 871-880. doi:10.1038/nature724

Wu, N., Zheng, B., Shaywitz, A., Dagon, Y., Tower, C., Bellinger, G., Shen, C. H., Wen, J., Asara, J., McGraw, T. E. et al. (2013). AMPK-dependent degradation of TXNIP upon energy stress leads to enhanced glucose uptake via GLUT1. *Mol. Cell* **49**, 1167-1175. doi:10.1016/j.molcel.2013.01.035

Wullschleger, S., Loewith, R. and Hall, M. N. (2006). TOR signaling in growth and metabolism. *Cell* **124**, 471-484. doi:10.1016/j.cell.2006.01.016

Zhang, Y., Gao, X., Saucedo, L. J., Ru, B., Edgar, B. A. and Pan, D. (2003). Rheb is a direct target of the tuberous sclerosis tumour suppressor proteins. *Nat. Cell Biol.* **5**, 578-581. doi:10.1038/ncb999

Zhang, P., Wang, C., Gao, K., Wang, D., Mao, J., An, J., Xu, C., Wu, D., Yu, H., Liu, J. O. et al. (2010). The ubiquitin ligase itch regulates apoptosis by targeting thioredoxin-interacting protein for ubiquitin-dependent degradation. *J. Biol. Chem.* **285**, 8869-8879. doi:10.1074/jbc.M109.063321

Zuckerman, R. and Cheasty, J. E. (1986). A 48 kDa protein arrests cGMP phosphodiesterase activation in retinal rod disk membranes. *FEBS Lett.* **207**, 35-41. doi:10.1016/0014-5793(86)80008-4